

New results and prospects for $b \rightarrow s \mu^+ \mu^-$ measurements

Presented at SM@LHC

Joel Butler, Fermilab, CMS

July 13, 2023

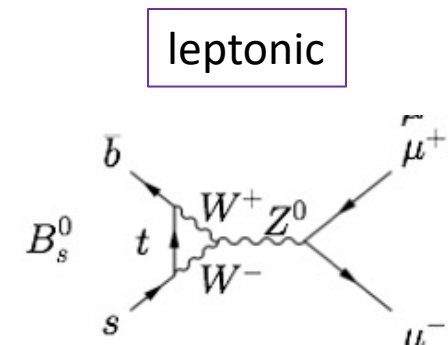
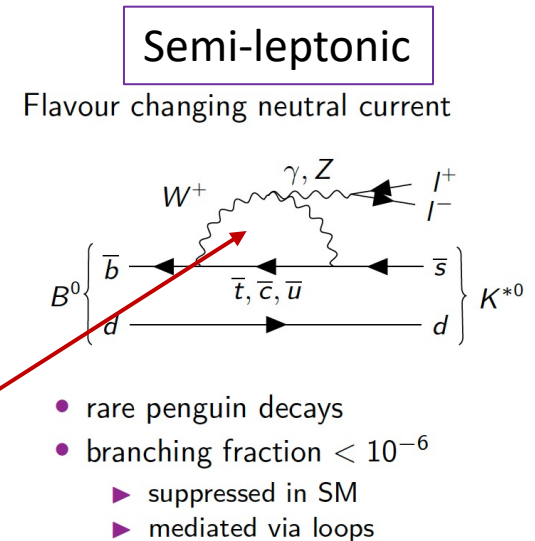
Outline

- Why $b \rightarrow s \mu^+ \mu^-$? The characteristics that make these decays promising ones for observing New Physics (NP)
 - “Light” treatment of Theory Framework for NP Studies
 - $B^0 \rightarrow K^{*0} \mu^+ \mu^-$
 - $B_s \rightarrow \phi \mu^+ \mu^-$
 - $\Lambda_b \rightarrow \Lambda (1520) (pK) \mu^+ \mu^-$, $\Lambda_b \rightarrow \Lambda \mu^+ \mu^-$
 - $B^0_{(s,d)} \rightarrow \mu^+ \mu^-$ (branching fraction and lifetime).
 - Conclusion
- Diagrammatic annotations:
- A right-facing curly bracket groups the first four decay modes ($B^0 \rightarrow K^{*0} \mu^+ \mu^-$, $B_s \rightarrow \phi \mu^+ \mu^-$, $\Lambda_b \rightarrow \Lambda (1520) (pK) \mu^+ \mu^-$, and $\Lambda_b \rightarrow \Lambda \mu^+ \mu^-$), with a blue arrow pointing to the text "semileptonic".
 - A blue arrow points from the text " $B^0_{(s,d)} \rightarrow \mu^+ \mu^-$ (branching fraction and lifetime)." to the text "leptonic".

An overview of recent experimental results

Why use $b \rightarrow s \mu^+ \mu^-$ to search for new physics

- To observe physics beyond the SM, i.e., New Physics (NP), need processes highly suppressed in SM
 - Here N_{SM} is part of the “background”, **so we want it to be small!**
- Transitions $b \rightarrow s \ell^+ \ell^-$ are forbidden at tree level in SM. They can only proceed via higher-order electroweak (loop, box) diagrams, which are very small.
 - These transitions constitute powerful probes for NP since new particles can appear in the loop**
- Observables that can reveal new physics are
 - Branching fractions, including differential BFs vs dimuon mass
 - Angular observables -- to locate a corner of phase space where NP stands out.
 - Ratio of branching fractions between decays with different flavors of leptons, i.e., for tests Lepton Universality (LU) **(discussed in the following talk)**
- Must have a reliable theory prediction with only small uncertainties in hadronic corrections for the $b \rightarrow s$ transition.
- Must be able to trigger and reconstruct the state with high efficiency and low backgrounds



Theory Framework

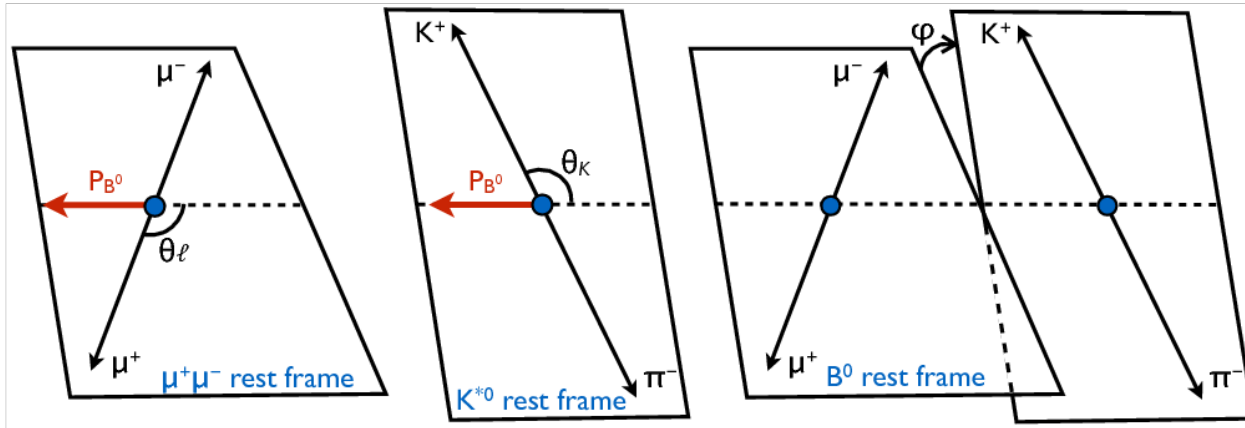
- SM and NP contributions to rare decays can be described by the effective Hamiltonian framework, which provides a model-independent description based on the Wilson coefficients of dimension 6 operators:

$$\mathcal{H}_{\text{eff}} = -\frac{4G_F}{\sqrt{2}}V_{tb}V_{ts}^*\frac{\alpha}{4\pi}\sum_i\left[(C_i^{\text{SM}}+\Delta C_i)O_i+\Delta C'_iO'_i\right],$$

- The most important operators for these decays are

$$\begin{array}{l} O_7 = \frac{1}{e}(\bar{s}\sigma_{\mu\nu}P_Rb)F^{\mu\nu}, \\ O_9 = (\bar{s}\gamma_\mu P_Lb)(\bar{\ell}\gamma^\mu\ell), \\ O_{10} = (\bar{s}\gamma_\mu P_Lb)(\bar{\ell}\gamma^\mu\gamma_5\ell), \\ O_S = m_b(\bar{s}P_Rb)(\bar{\ell}\ell), \\ O_P = m_b(\bar{s}P_Rb)(\bar{\ell}\gamma_5\ell), \end{array} \quad \begin{array}{l} O'_7 = \frac{1}{e}(\bar{s}\gamma_\mu P_Lb)F^{\mu\nu}, \\ O'_9 = (\bar{s}\gamma_\mu P_Rb)(\bar{\ell}\gamma^\mu\ell), \\ O'_{10} = (\bar{s}\gamma_\mu P_Rb)(\bar{\ell}\gamma^\mu\gamma_5\ell), \\ O'_S = m_b(\bar{s}P_Lb)(\bar{\ell}\ell), \\ O'_P = m_b(\bar{s}P_Lb)(\bar{\ell}\gamma_5\ell). \end{array}$$

- The operators $O_{9,10}$ are SM operators. ΔC_i are deviations to the SM coefficients.
- The primed operators $O'_{9,10}$ are NP operators. $\Delta C'_i$ are deviations to the caused by the NP operators
- The strategy is to compare the values observed in the data for these coefficients with the SM predictions.



q^2 is the invariant mass squared of the dimuon

- The $K^+\pi^-$ from the $K^*(890)$ are in a P-wave. An S-wave contribution to the $K^+\pi^-$ mass region acts as a contamination to the $K^*(890)$ angular observables and must be accounted for in the fits.

P-wave

$$\frac{1}{d(\Gamma + \bar{\Gamma})/dq^2} \frac{d^4(\Gamma + \bar{\Gamma})}{dq^2 d\Omega} \Big|_P = \frac{9}{32\pi} \left[\frac{3}{4}(1 - F_L)\sin^2\theta_K + F_L\cos^2\theta_K + \frac{1}{4}(1 - F_L)\sin^2\theta_K \cos 2\theta_l \right. \\ \left. - F_L\cos^2\theta_K \cos 2\theta_l + S_3\sin^2\theta_K \sin^2\theta_l \cos 2\phi + S_4\sin 2\theta_K \sin 2\theta_l \cos \phi + S_5\sin 2\theta_K \sin \theta_l \cos \phi \right. \\ \left. + \frac{4}{3}A_{FB}\sin^2\theta_K \cos \theta_l + S_7\sin 2\theta_K \sin \theta_l \sin \phi + S_8\sin 2\theta_K \sin 2\theta_l \sin \phi + S_9\sin^2\theta_K \sin^2\theta_l \sin 2\phi \right],$$

P-wave + S-wave

$$\frac{1}{d(\Gamma + \bar{\Gamma})/dq^2} \frac{d^4(\Gamma + \bar{\Gamma})}{dq^2 d\Omega} \Big|_{S+P} = (1 - F_S) \frac{1}{d(\Gamma + \bar{\Gamma})/dq^2} \frac{d^4(\Gamma + \bar{\Gamma})}{dq^2 d\Omega} \Big|_P + \frac{3}{16\pi} F_S \sin^2\theta_l + \frac{9}{32\pi} (S_{11} + S_{13} \cos 2\theta_l) \cos \theta_K \\ + \frac{9}{32\pi} (S_{14} \sin 2\theta_l + S_{15} \sin \theta_l) \sin \theta_K \cos \phi + \frac{9}{32\pi} (S_{16} \sin \theta_l + S_{17} \sin 2\theta_l) \sin \theta_K \sin \phi,$$

F_L is the longitudinal polarization $F_L = S_1$; the forward-backward asymmetry $A_{FB} = 3/4S_6$

Special Considerations

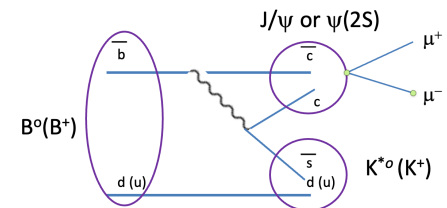
- q^2 interval (dimuon mass²) restrictions: the dimuon can be resonant, i.e., J/ψ or ψ' . These processes are **dominated by $b \rightarrow c$ transitions**, with the virtual W going into a c - s final state. This results in ψK^{*0} with J/ψ or $\psi' \rightarrow \mu^+ \mu^-$. These q^2 intervals must be excluded from the s - $b \ell \ell$ amplitude analysis. **The resonant final states enter the analysis process, however as control, calibration, and monitoring channels.**

- The q^2 intervals are based on the q^2 resolution of each experiment, which determines bin width and migration

- There are still theoretical uncertainties in some of the coefficients from QCD. “Optimized” observables for which the leading $B^0 \rightarrow K^{*0}$ form-factor uncertainties cancel, can be built from F_L , A_{FB} , and S_3 – S_9 . Examples of such optimized observables include the P'_i series of observables. The notation used is from

- Kruger, Frank and Matias, Joaquim, Phys. Rev. D71 (2005) 094009, arXiv:hep-ph/0502060. and
- S. Descotes-Genon, J. Matias, M. Ramon, and J. Virto, JHEP 01 (2013) 048, arXiv:1207.2753.

Resonant dimuons



The optimized observables commonly used are:

$$P_1 = \frac{2S_3}{1 - F_L},$$

$$P_2 = \frac{2}{3} \frac{A_{FB}}{1 - F_L},$$

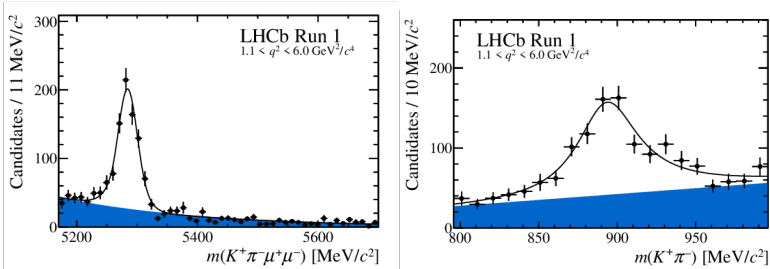
$$P_3 = \frac{-S_9}{1 - F_L} \text{ and}$$

$$P'_{4,5,6,8} = \frac{S_{4,5,7,8}}{\sqrt{F_L(1 - F_L)}}.$$

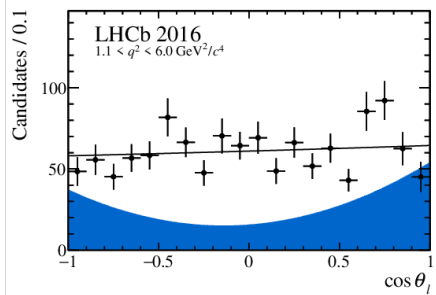
$B^0 \rightarrow K^{*0}(\rightarrow K^+\pi^-)\mu^+\mu^-$ from LHCb

PRL 125, 011802 (2020)

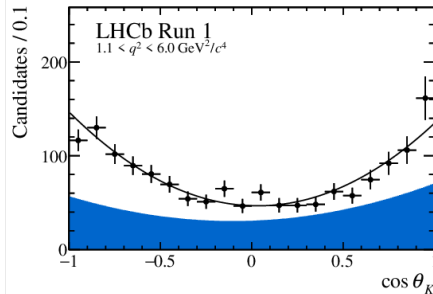
4.7 fb⁻¹



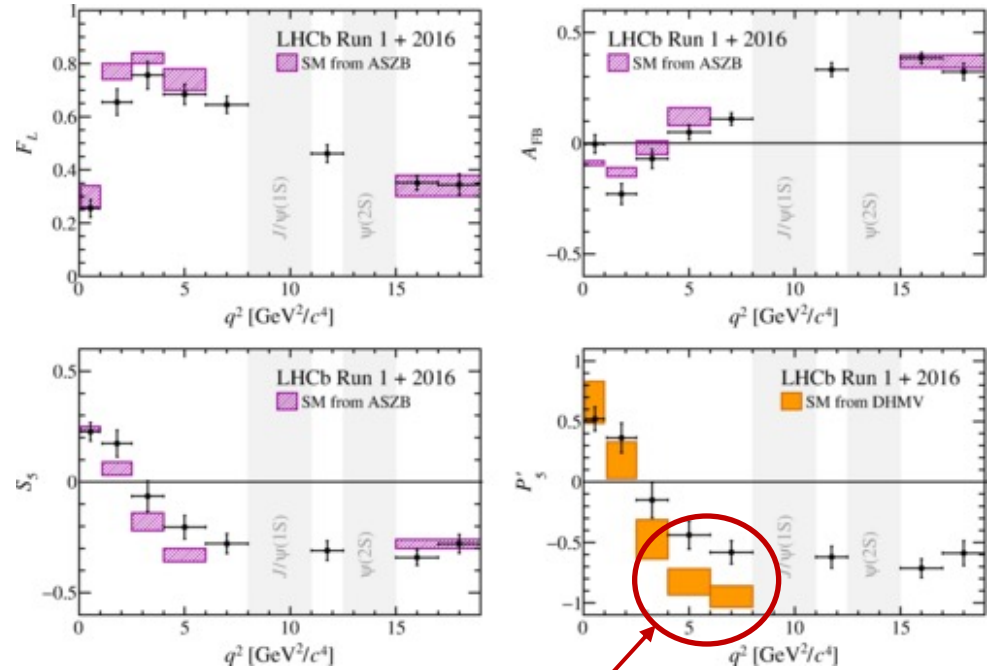
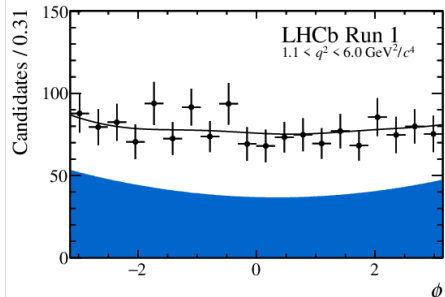
$\cos \theta_\ell$



$\cos \theta_K$



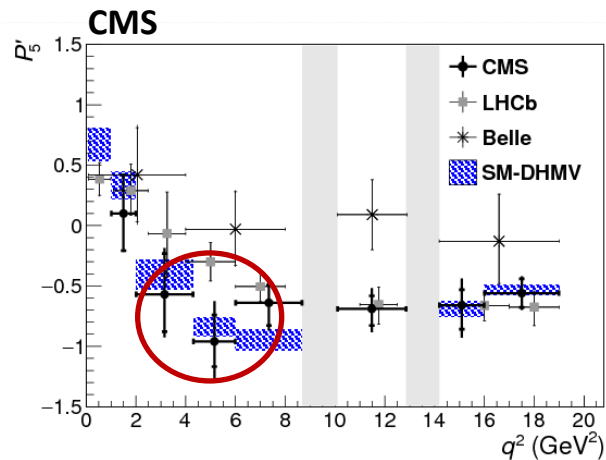
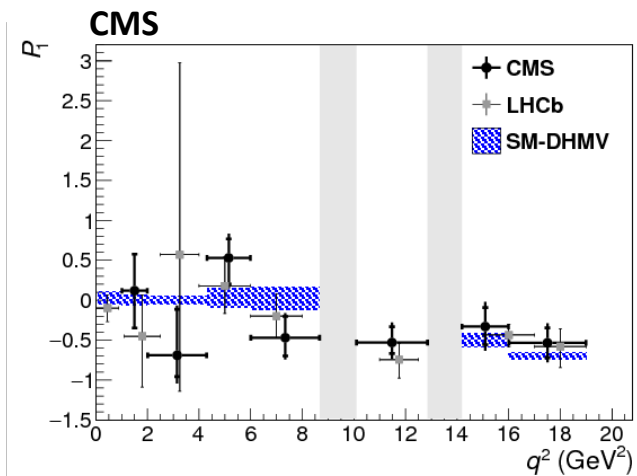
ϕ



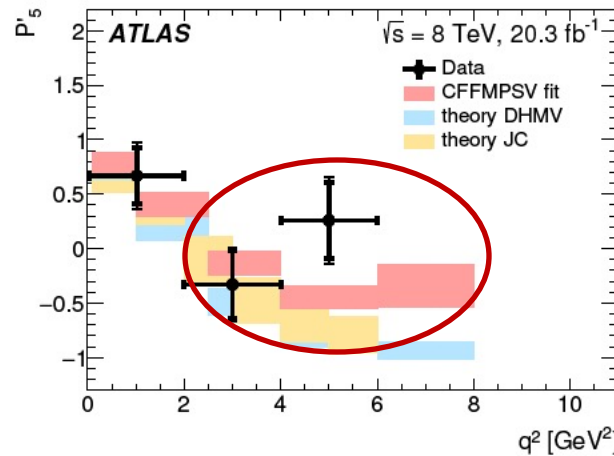
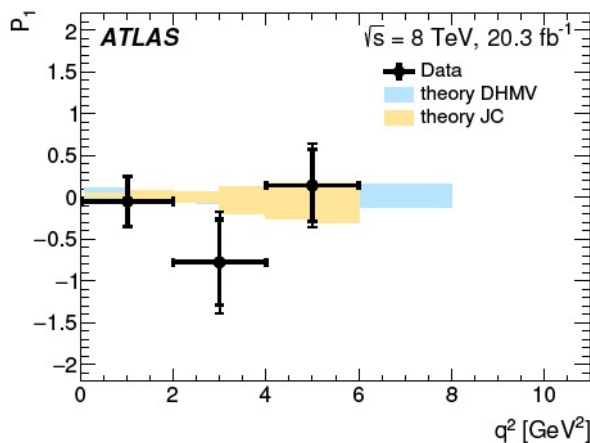
- This shows the small tension in P'_5 that has caused excitement. Note the excluded regions in q^2 .

$B^0 \rightarrow K^{*0}(890)(\rightarrow K^+\pi^-)\mu^+\mu^-$ from CMS and ATLAS

Similar distributions from CMS and ATLAS.



[Physics Letters B, Vol. 781,](#)
10 June 2018, Pages 517-541



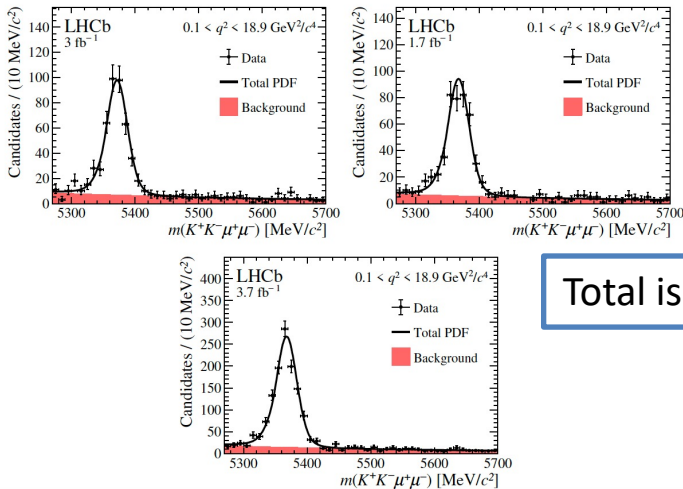
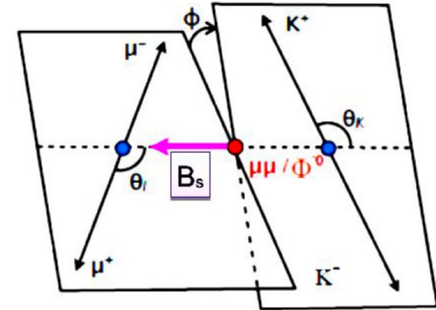
[JHEP 10 \(2018\) 047](#)

$B_s \rightarrow \phi(k^+k^-)\mu^+\mu^-$ from LHCb

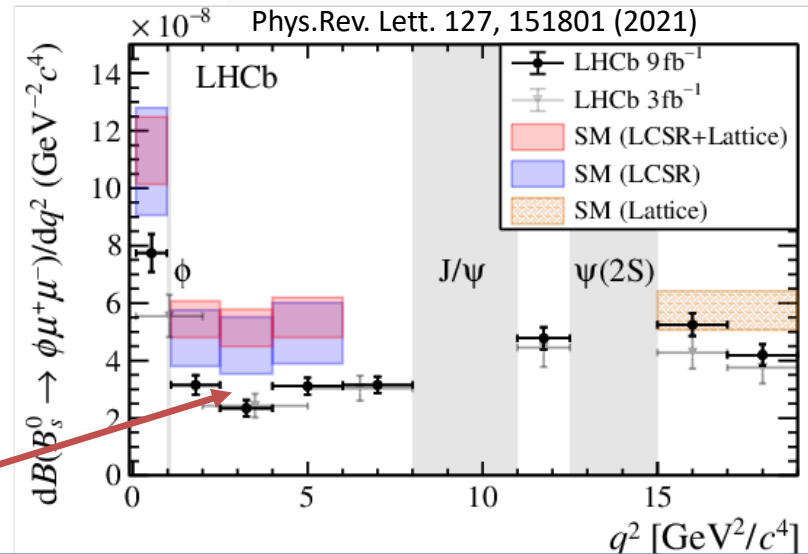
[Phys. Rev. Lett. 127 \(2021\) 151801](#), [JHEP 2111 \(2021\) 043](#)

$$\frac{1}{d(\Gamma + \bar{\Gamma})/dq^2} \frac{d^3(\Gamma + \bar{\Gamma})}{d\cos\theta_l d\cos\theta_K d\phi} = \frac{9}{32\pi} \left[\frac{3}{4}(1 - F_L) \sin^2\theta_K \left(1 + \frac{1}{3} \cos 2\theta_l\right) + F_L \cos^2\theta_K (1 - \cos 2\theta_l) + S_3 \sin^2\theta_K \sin^2\theta_l \cos 2\phi + S_4 \sin 2\theta_K \sin 2\theta_l \cos \phi + A_5 \sin 2\theta_K \sin \theta_l \cos \phi + \frac{4}{3} A_{\text{FB}}^{\text{CP}} \sin^2\theta_K \cos \theta_l + S_7 \sin 2\theta_K \sin \theta_l \sin \phi + A_8 \sin 2\theta_K \sin 2\theta_l \sin \phi + A_9 \sin^2\theta_K \sin^2\theta_l \sin 2\phi \right],$$

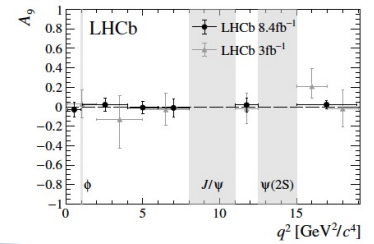
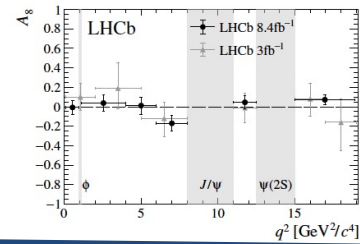
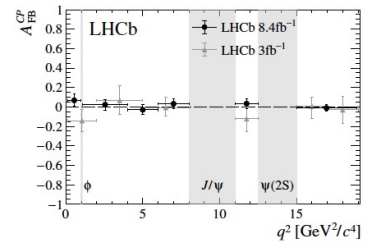
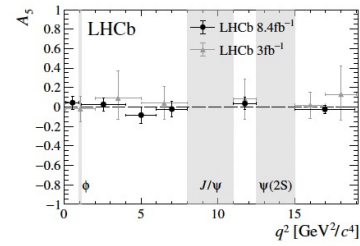
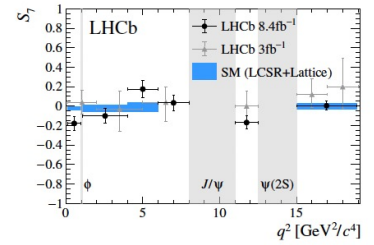
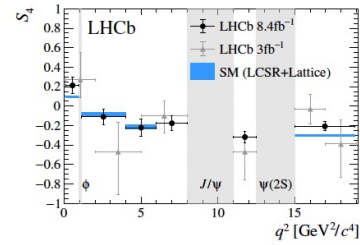
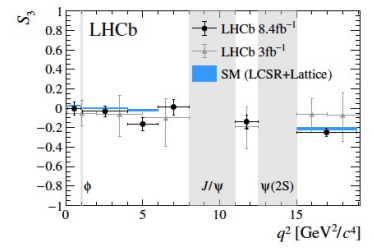
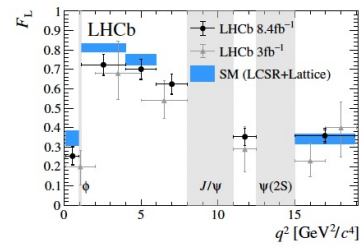
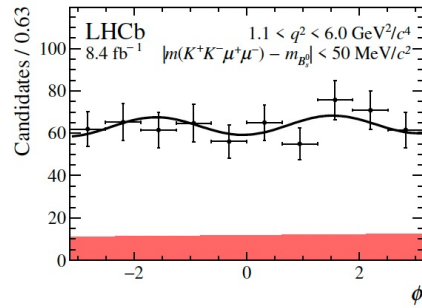
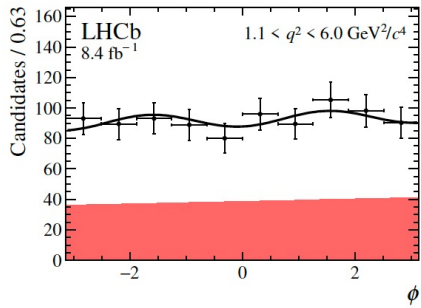
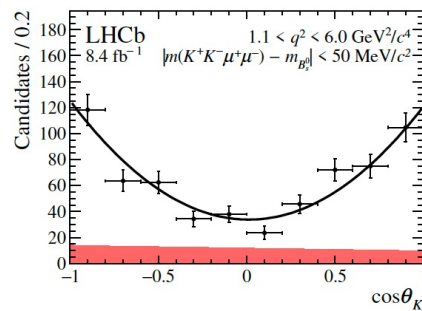
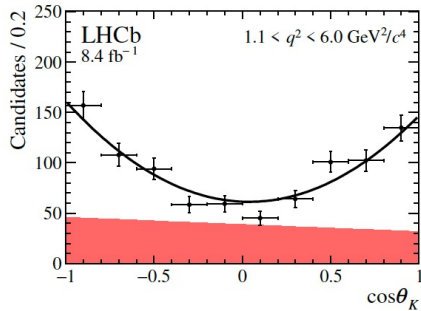
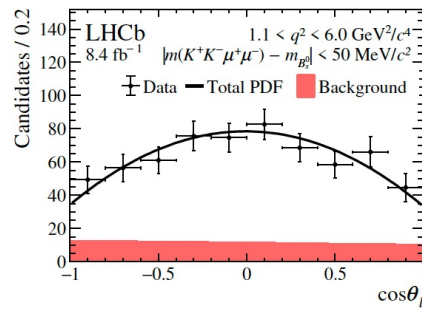
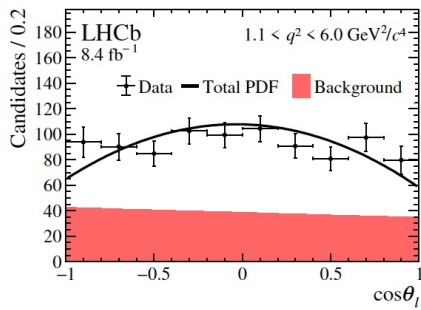
F_L and $S_{3,4,5}$ are CP averages and $A_{\text{FB}}^{\text{CP}}$ and $A_{5,8,9}$ are CP asymmetries. A_8 and A_9 are T-odd CP asymmetries (near 0 in SM)



Total is 8.4 fb^{-1}



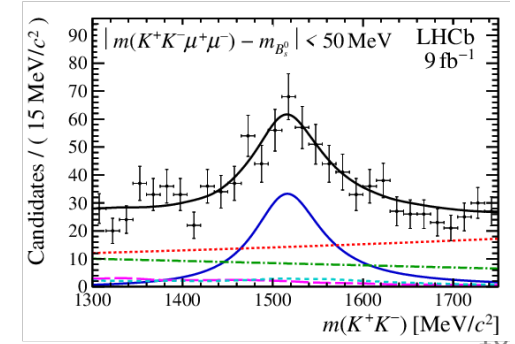
In the q^2 region between 1.1 and 6.0 GeV^2/c^4 , the measurement is found to lie 3.6 standard deviations below a standard model prediction based on a combination of light cone sum rule and lattice QCD calculations. $\mathcal{B}(B^0 \rightarrow \phi(\mu^+\mu^-)) \rightarrow (8.14 \pm 0.21 \pm 0.16 \pm 0.03 \pm 0.39) \times 10^{-7}$.



- $B_s \rightarrow f_2'(1525) \mu^+ \mu^-$ (f_2' is a spin 2 meson)

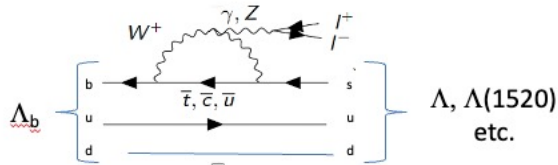
$$B(B_s \rightarrow f_2' \mu^+ \mu^-) = (1.57 \pm 0.19 \pm 0.06 \pm 0.06 \pm 0.08) \times 10^{-7}$$

Statistical significance of 9 standard deviations and the resulting branching fraction agrees with SM predictions.

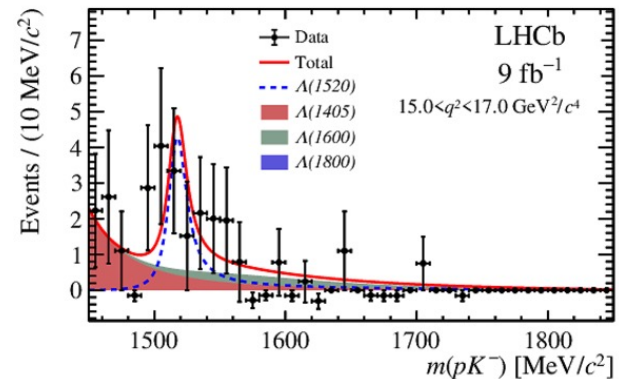
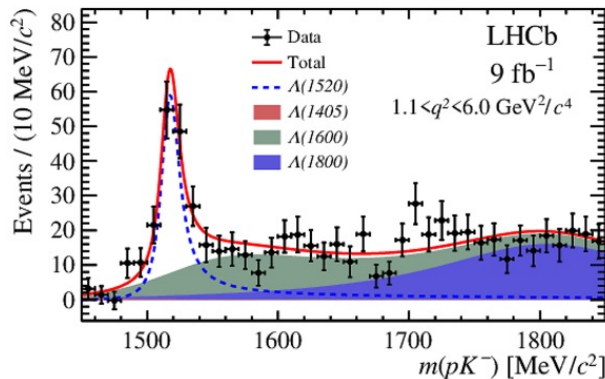
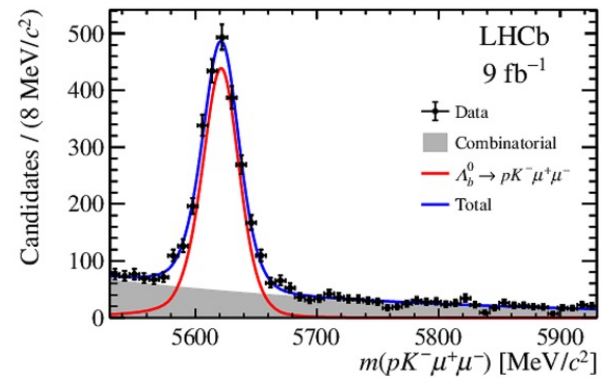
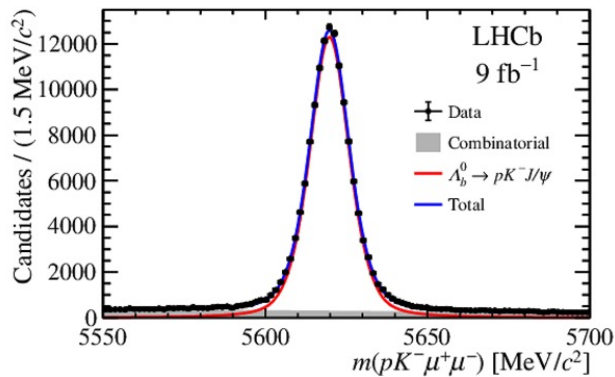


$\Lambda_b \rightarrow \Lambda(1520) (pK) \mu^+ \mu^-$ (LHCb)

[arXiv:2302.08262](https://arxiv.org/abs/2302.08262)

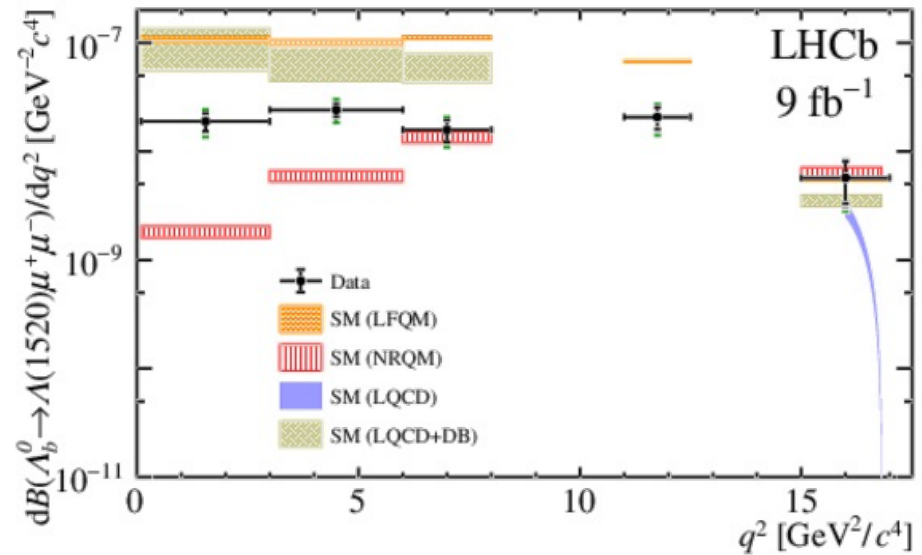
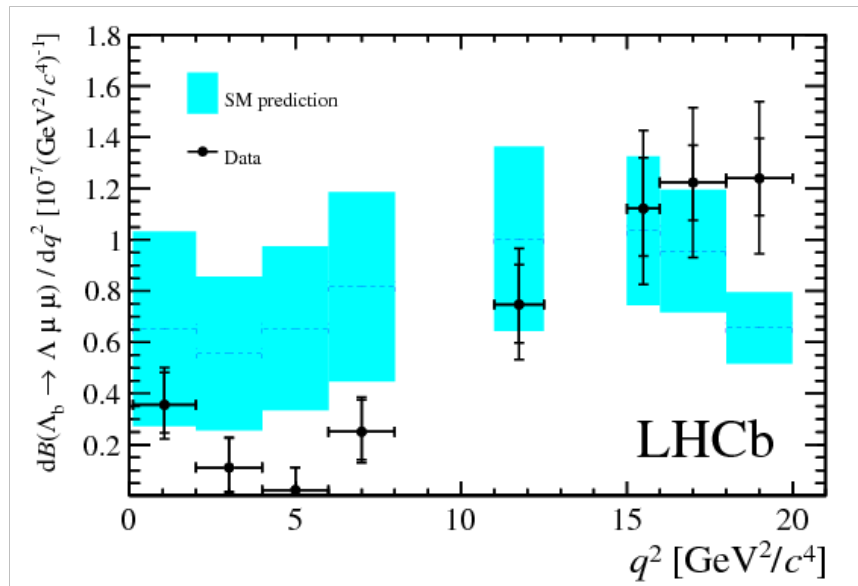


$\Lambda(1520): 0(3/2)^-$
 $M = 1519 \text{ MeV}, \Gamma = 16 \text{ MeV}$
 $\mathcal{B}(pK) = 22.5\%$



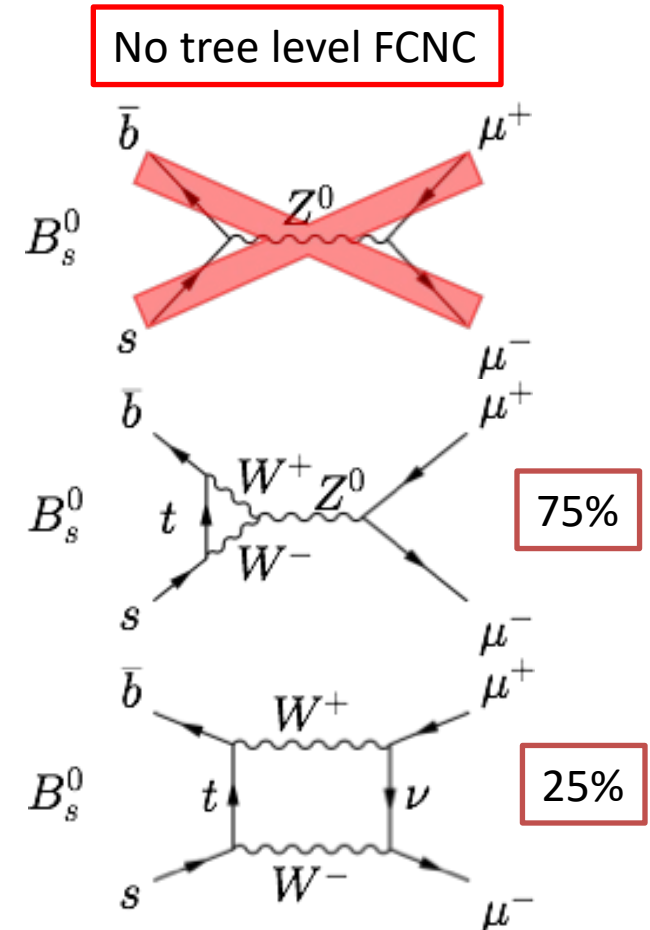
$\Lambda_b \rightarrow \Lambda, \Lambda(1520) (\text{pK}) \mu^+ \mu^-$ from LHCb

[arXiv:2302.08262](https://arxiv.org/abs/2302.08262)



$B_{s,d} \rightarrow \mu^+ \mu^-$ in the Standard Model

- In the Standard Model, $B_{s,d} \rightarrow \mu^+ \mu^-$ decays are **highly suppressed**:
 - Flavor Changing Neutral Current (FCNC) processes in SM are forbidden at tree level but can proceed through Z-penguin, and box diagrams
 - Helicity suppressed: $[m_\mu/m_B]^2$
 - Makes $B_{s,d} \rightarrow e^+ e^-$ inaccessible
 - CKM suppressed by $|V_{tq}|^2$:
 - $B^0 \rightarrow \mu^+ \mu^-$ further Cabibbo suppressed by $|V_{td}/V_{ts}|^2$, relative to B_s , which gives about a factor of 20 lower branching fraction.
 - Slightly compensated in rate since B^0 has twice the cross section of B_s .
- Resulting **tiny branching fractions**, but rather robust SM theory predictions are available



Standard Model Prediction simplified

Decay constant

Proxy for full amplitude

$$\bar{B}_{q\ell} = \frac{|N|^2 M_{B_q}^3 f_{B_q}^2}{8\pi\Gamma_H^q} \beta_{q\ell} r_{q\ell}^2 |C_A(\mu_b)|^2 + \mathcal{O}(\alpha_{em})$$

$$N = V_{ib}^* V_{iq} G_F^2 M_W^2 / \pi^2 \quad r_{q\ell} = 2m_\ell / M_{B_q} \quad \beta_{q\ell} = \sqrt{1 - r_{q\ell}^2}$$

Flavor mixing in the SM produces two mass eigenstates, denoted as $B_{s,dL}^0$ and $B_{s,dH}^0$, where (L,H → light, heavy), which are CP-even and CP-odd, respectively. A dimuon can be shown to be CP odd, so the parent of the decay is also CP odd. The widths (lifetimes) of these states are $\Gamma_L(\tau_L)$ and $\Gamma_H(\tau_H)$, respectively. These two widths (lifetimes) are nearly identical for B_d but quite different for B_s

The SM predictions for the branching fractions are:

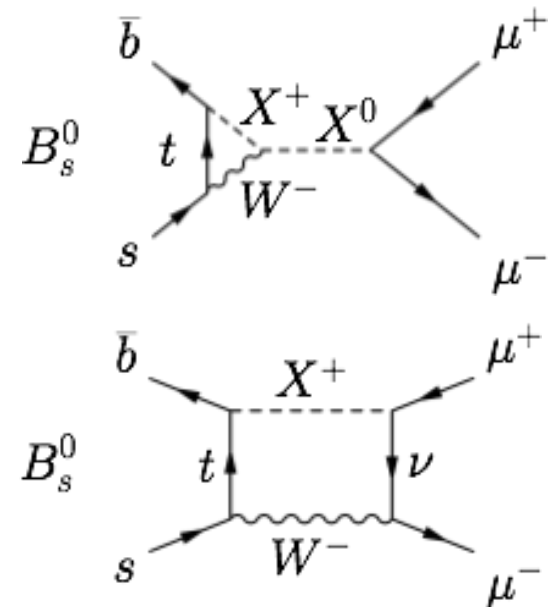
$$\mathcal{B}(B_s^0 \rightarrow \mu^+\mu^-) = (3.66 \pm 0.14) \times 10^{-9}$$

$$\mathcal{B}(B^0 \rightarrow \mu^+\mu^-) = (1.03 \pm 0.05) \times 10^{-10}$$

These predictions include next-to-leading order corrections of EW origin and next-to-next-to-leading order QCD corrections. The largest contribution to the theoretical uncertainty is from the determination of the CKM matrix element values, in particular $|V_{cb}|$.

$B_{s,d} \rightarrow \mu^+ \mu^-$: the potential for New Physics

- Loop diagram + Suppressed SM + Theoretically clean
→ An excellent place to look for new physics.
- Sensitive to extended Higgs sectors
⇒ Constrains NP parameter spaces.
- A few NP examples:
 - 2HDM: $B \propto \tan^4 \beta$, and $m(H^+)$
 - CMSSM/mSUGRA: $B \propto \tan^6 \beta$
 - Leptoquarks



Any difference in branching fraction from SM could provide a strong indication of new physics.

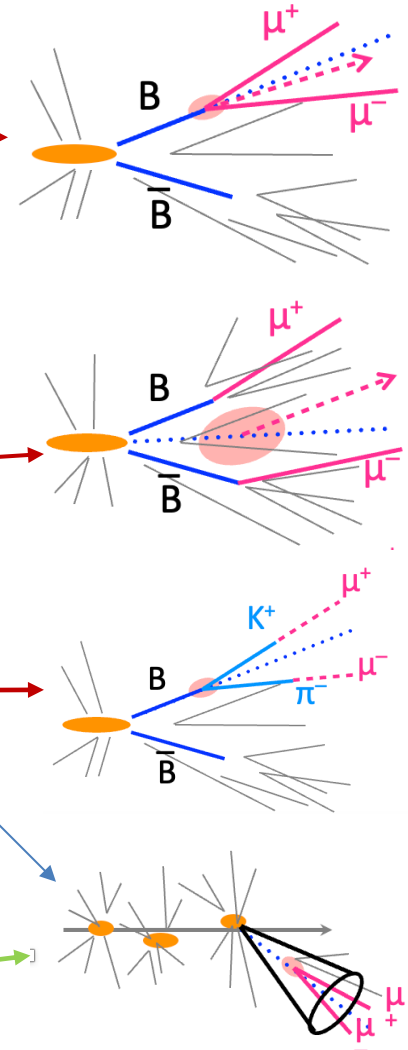
Measurement of the $B_s \rightarrow \mu^+\mu^-$ decay properties and search for the $B_d \rightarrow \mu^+\mu^-$ from CMS [Phys. Lett. B 842 \(2023\) 137955](#)

- **The $B_{s,d} \rightarrow \mu^+\mu^-$ signal**

- two **isolated, opposite signed** muons forming a good displaced vertex; dimuon momentum aligned with flight direction from primary and secondary vertex; dimuon mass consistent with $M(B_{s,d})$ (in the unblinding process)

- **Background sources**

- two semileptonic B decays
- one semileptonic B + a misidentified hadron
- rare background from single B meson decays: e.g. $B \rightarrow K\pi/KK$ (*peaking*), $B_s \rightarrow K^-\mu^+\nu$, $\Lambda_b \rightarrow p\mu\nu$ (*not peaking*), where hadrons either appear to be muons through decays or “punch-through”



Powerful background suppression reached by **muon quality**, **well-reconstructed secondary vertex**, muon and B isolation, **pointing angle**, and **$M(\mu\mu)$ resolution**.

Normalization using $B^+ \rightarrow \psi(\mu^+\mu^-)K^+$

$$\mathcal{B}(B_s^0 \rightarrow \mu^+\mu^-) = \mathcal{B}(B^+ \rightarrow J/\psi K^+) \frac{N_{B_s^0 \rightarrow \mu^+\mu^-}}{N_{B^+ \rightarrow J/\psi K^+}} \frac{\varepsilon_{B^+ \rightarrow J/\psi K^+}}{\varepsilon_{B_s^0 \rightarrow \mu^+\mu^-}} \frac{f_u}{f_s}$$

$$\mathcal{B}(B_d^0 \rightarrow \mu^+\mu^-) = \mathcal{B}(B^+ \rightarrow J/\psi K^+) \frac{N_{B_d^0 \rightarrow \mu^+\mu^-}}{N_{B^+ \rightarrow J/\psi K^+}} \frac{\varepsilon_{B^+ \rightarrow J/\psi K^+}}{\varepsilon_{B_d^0 \rightarrow \mu^+\mu^-}} \frac{f_u}{f_d}$$

N_x number of candidates of decay X from fit

ε_x is the full selection efficiency from MC

f_u, f_d, f_s are the production fractions for $B^+, B^0,$ and B_s mesons, respectively

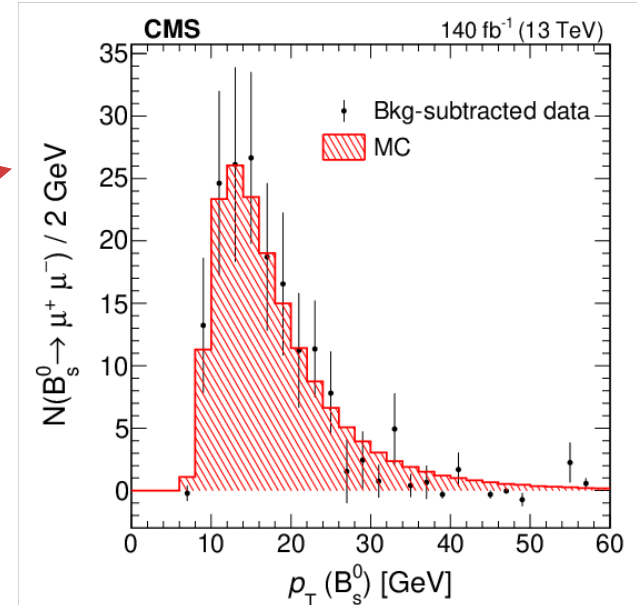
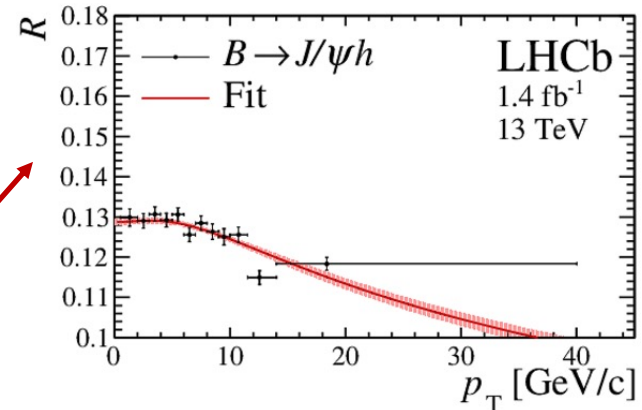
The production fractions were thought of as constants, independent of P_T and η , with $f_u = f_d$ via isospin.

The external inputs to the calculation of the branching ratios were

But LHCb establishes that there is a P_T and center of mass energy dependence, but no η dependence **Phys. Rev. D 104, 032005**. We use the P_T distribution observed in pir CMS measurement to compute an effective f_s/f_d ratio.

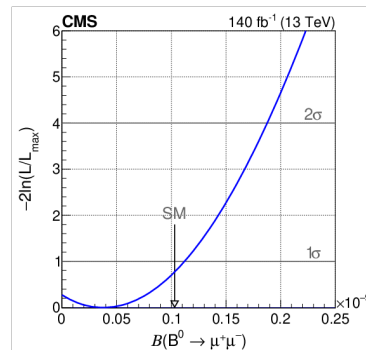
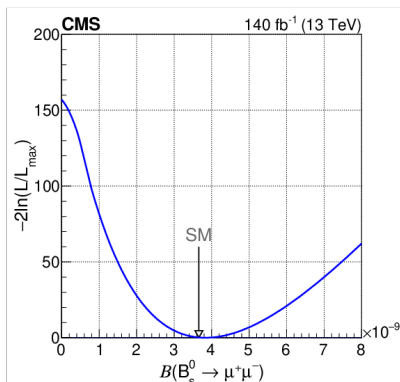
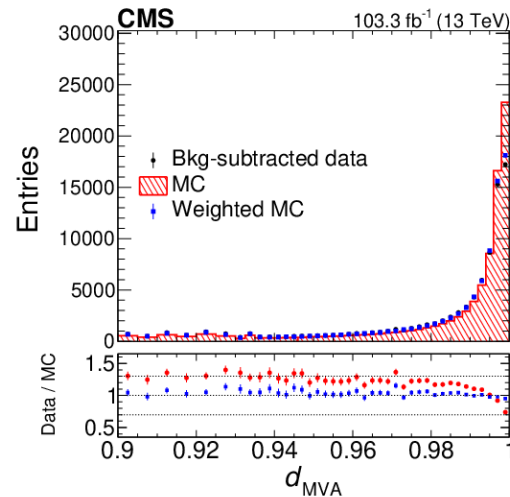
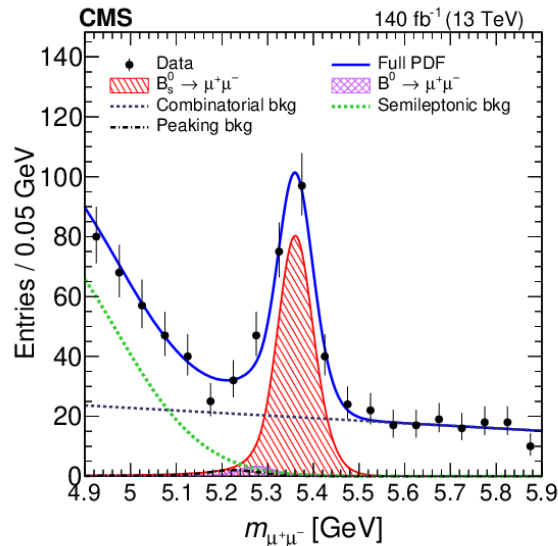
The external inputs then are:

- $\mathcal{B}(B^+ \rightarrow J/\psi K^+) = (1.020 \pm 0.019) \times 10^{-3}$,
- $\mathcal{B}(J/\psi \rightarrow \mu^+\mu^-) = (5.961 \pm 0.033) \times 10^{-2}$, and
- $f_s/f_u = 0.231 \pm 0.008$.

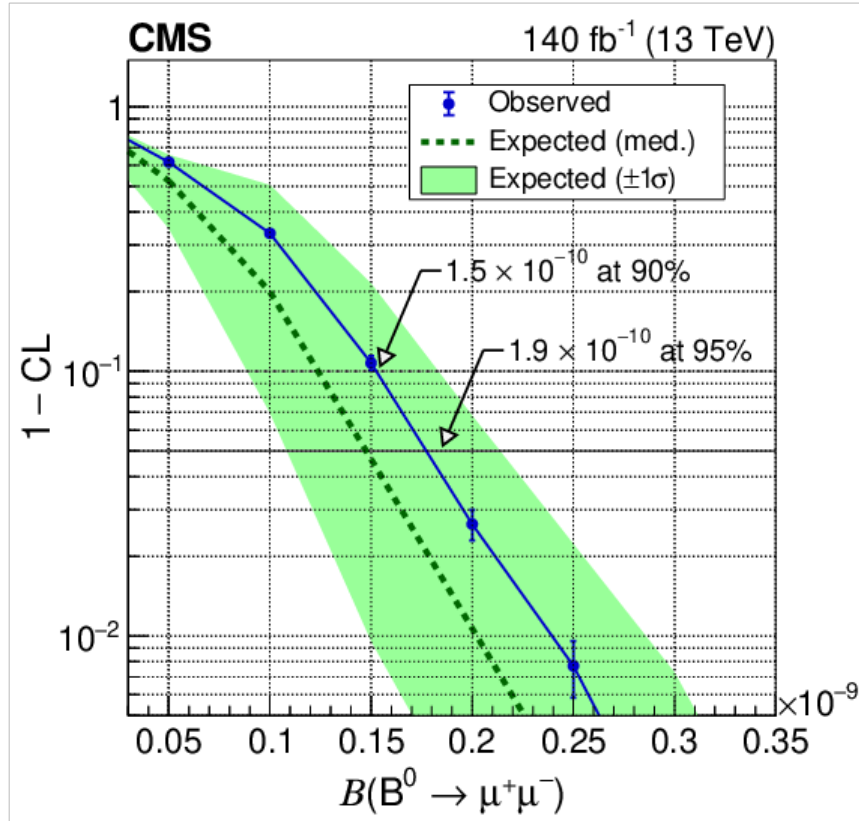
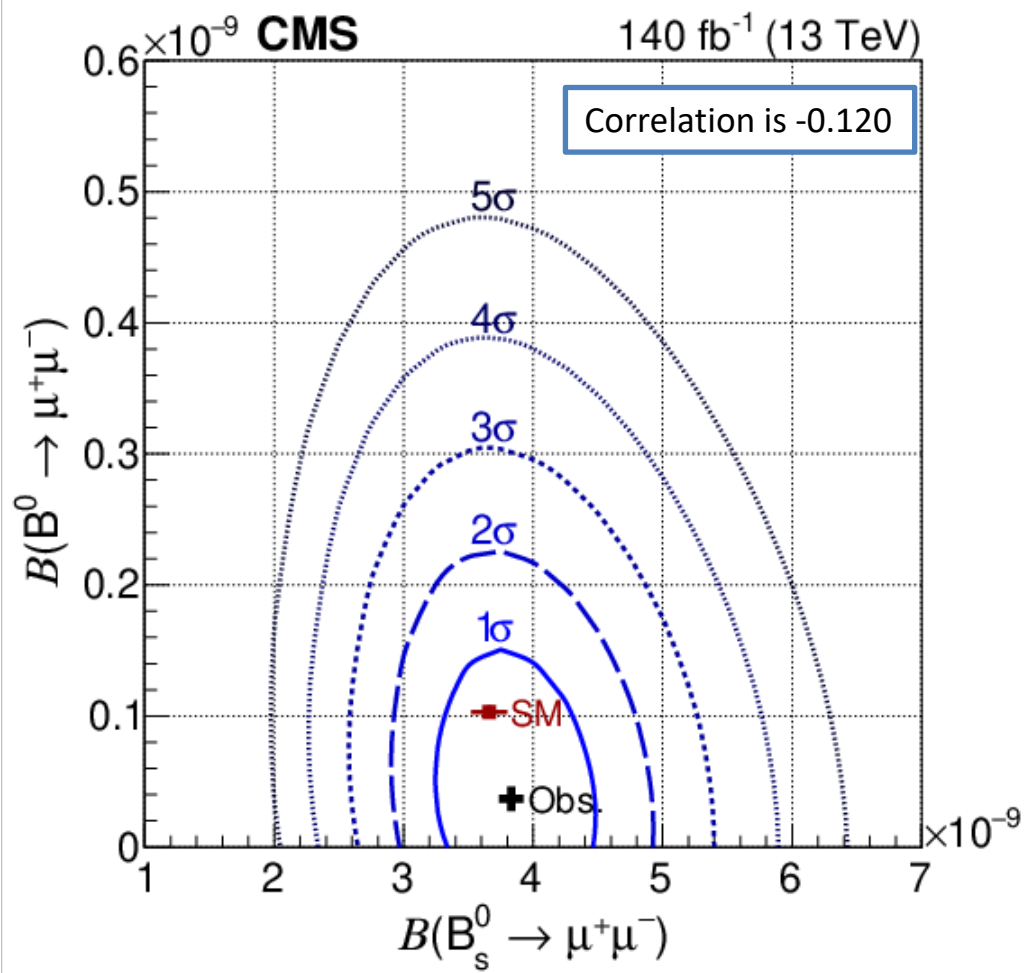


Most Recent Result – CMS

- Based on 140 fb^{-1} from 2016, 2017, 2018, [Phys. Lett. B 842 \(2023\) 137955](#)



- Blinded analysis
- Same muon MVA, with minor change in cut on MVA output
- New Analysis MVA using XGBoost library
 - Optimized using signal Monte Carlo and background from data sidebands
 - K-folding used to avoid including possible correlations
- Unbinned ML fit to dimuon mass distribution, which includes model for signal, combinatoric background, and peaking background blinded region.
- Normalization using $B^+ \rightarrow J/\psi K^+$
 - Also used to get efficiencies, resolutions, etc
- Improvements in analysis sensitivity
 - Relaxed preselection (let MVA do it work)
 - Developed new discriminating observables
 - Added much more background data to the training model
 - Used a more advanced machine learning algorithm



Upper limits on $B^0 \rightarrow \mu^+\mu^-$ branching fraction using the CL_s method.

$$B(B_s^0 \rightarrow \mu^+\mu^-) = \left[3.83_{-0.36}^{+0.38} \text{ (stat)} \right]_{-0.16}^{+0.19} \text{ (syst)} \left[\frac{f_s}{f_u} \right]_{-0.13}^{+0.14} \times 10^{-9},$$

$$B(B^0 \rightarrow \mu^+\mu^-) = \left[0.37_{-0.67}^{+0.75} \text{ (stat)} \right]_{-0.09}^{+0.08} \text{ (syst)} \times 10^{-10}.$$

$$B(B^0 \rightarrow \mu^+\mu^-) < 1.5 \times 10^{-10} \text{ at 90\% CL,}$$

$$B(B^0 \rightarrow \mu^+\mu^-) < 1.9 \times 10^{-10} \text{ at 95\% CL,}$$

The result can be rescaled if the averaged value of f_s/f_u should change and the systematic uncertainty is separated out so it can be recomputed

Lifetime of B_{sH}

A dimuon from a spin 0^- state is CP odd, so the parent of the decay is CP odd. The widths (lifetimes) of these states are called $\Gamma_L (\tau_L)$ and $\Gamma_H (\tau_H)$, respectively. These two widths (lifetimes) are nearly identical for B_d but quite different for B_s

$$\tau_{B_s^0 \rightarrow \mu^+ \mu^-} \equiv \frac{\int_0^\infty t \langle \Gamma (B_s^0 \rightarrow \mu^+ \mu^-) \rangle dt}{\int_0^\infty \langle \Gamma (B_s^0 \rightarrow \mu^+ \mu^-) \rangle dt}$$

$$= \frac{\tau_{B_s^0}}{1 - y_s^2} \left[\frac{1 + 2\mathcal{A}_{\Delta\Gamma} y_s + y_s^2}{1 + \mathcal{A}_{\Delta\Gamma} y_s} \right],$$

$$y_s \equiv \frac{\Delta\Gamma_s}{2\Gamma_s}, \quad \mathcal{A}_{\Delta\Gamma} \equiv \frac{R_H^{\mu^+ \mu^-} - R_L^{\mu^+ \mu^-}}{R_H^{\mu^+ \mu^-} + R_L^{\mu^+ \mu^-}},$$

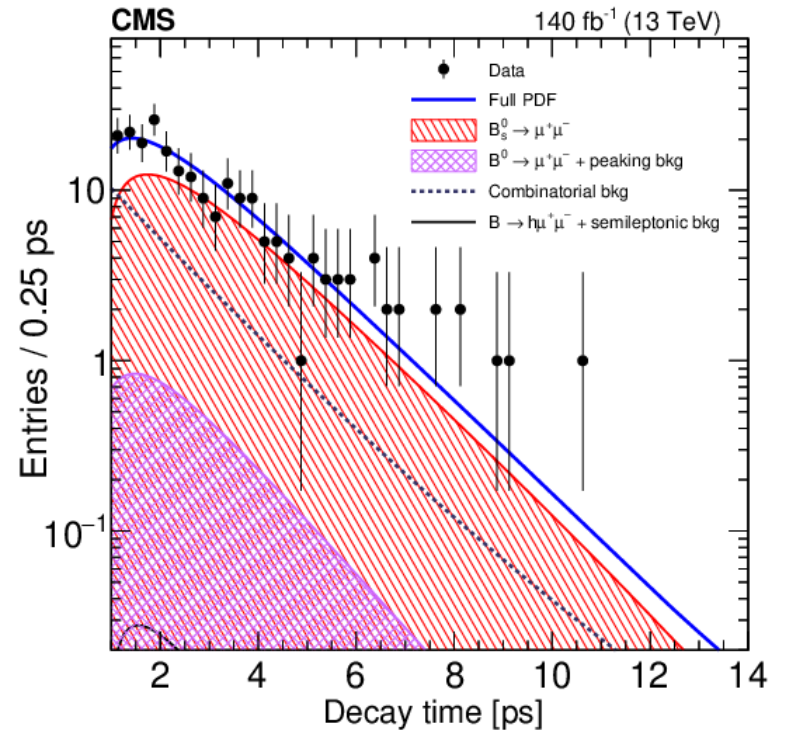
$\mathcal{A}_{\Delta\Gamma}$ can vary from +1 to -1. $\mathcal{A}_{\Delta\Gamma} = 1$ in the SM
And is an observable for NP

From flavor-specific hadronic decays

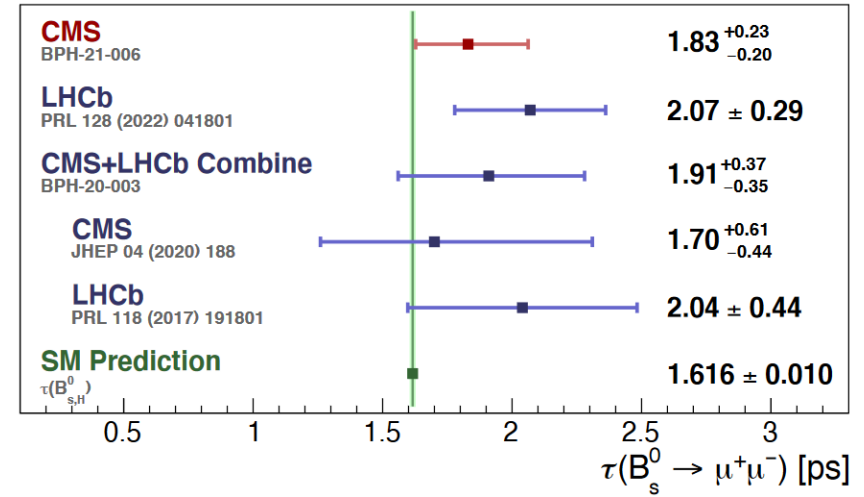
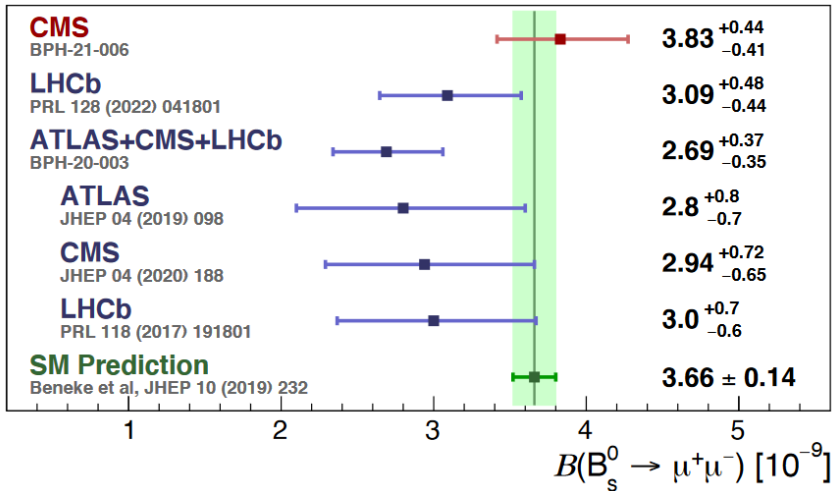
$$\tau (B_{sH}) = 1.609 \pm 0.010 \text{ ps}, \quad \tau (B_{sL}) = 1.413 \pm 0.006 \text{ ps},$$

This measurement: $\tau = 1.83^{+0.23}_{-0.20} \text{ (stat)} \ ^{+0.04}_{-0.04} \text{ (syst)} \text{ ps.}$

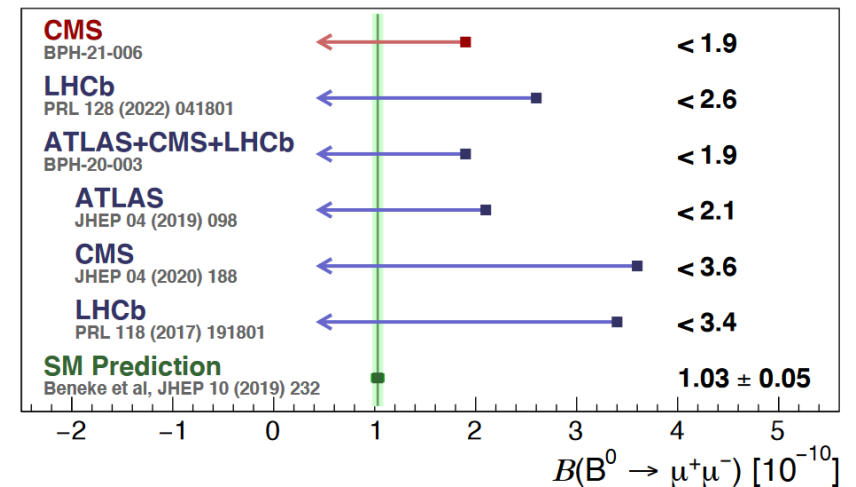
More statistics needed before any conclusion relative to NP can be made



Summary of World Data



- The CMS result uses 140 fb^{-1} from 2016, 2017, and 2018
- Compared with previous CMS measurement, the relative uncertainty is reduced from 23% to 11%
- CMS is about 1.2 standard deviations higher than LHCb
- There is some tension with previously combined result, ATLAS+CMS+LHCb in plot



Prospects for $b \rightarrow s \mu^+ \mu^-$ decays

- A large amount of work is being done on these channels and much progress has been made in last few years
 - New decay channels have been opened up, especially by LHCb, but some are accessible to ATLAS and CMS
- Whether or not any current hints survive, this path of searching for NP will remain promising and should be pursued
 - We have not even done all the analysis with data from Run 1 and 2, with only a few measurements using the full luminosity available and some are not started
 - We will have 2-3x more data by the end of Run 3 and 20x more by the end of the HL-LHC, bringing new decays and observables to the fore
 - It will be challenging to maintain the data quality because of radiation damage and aging and also pileup
- Theoretical predictions need to be improved
 - Issues such as f_s/f_d will begin to limit the precision
- Experiments can also help reduce uncertainties, e.g., a precision measurement of an absolute B_s branching fraction from BELLE II/KEK-B running on the $Y(5S)$ would allow us to use it in the normalization

There are many opportunities to look for new physics in these decays. Recently, we saw what a discovery could look like. We should not overlook this promising path to New Physics!

Thank you for your attention! I will be glad to try to answer questions and hear your comments.

Backup Slides

CMS Trigger for $B \rightarrow \mu^+ \mu^-$ Analysis

“The events used in this analysis were collected with a set of dimuon triggers designed to select events with :

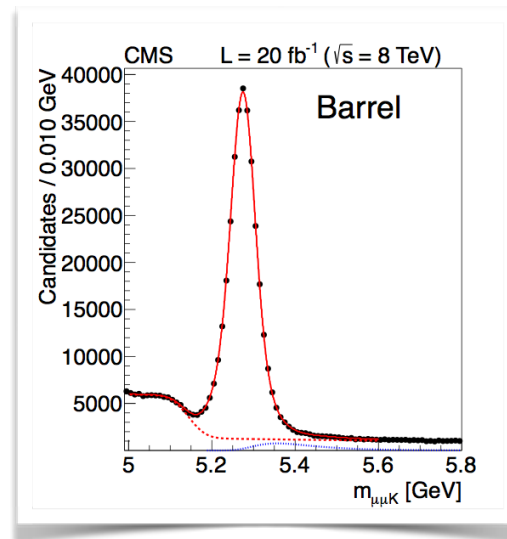
$$B \rightarrow \mu^+ \mu^-, B^+ \rightarrow J/\psi K^+, \text{ and } B_s^0 \rightarrow J/\psi \phi(1020)$$

To achieve an acceptable trigger rate, the **first-level trigger** required two high-quality oppositely charged muons restricted to $|\eta| < 1.5$.

At the **high-level trigger**, a high-quality dimuon secondary vertex (SV) was required and the events were restricted to mass ranges of $4.5\text{--}6.0\text{ GeV}$ and $2.9\text{--}3.3\text{ GeV}$ for the B and J/ψ mesons, respectively. The J/ψ triggers additionally required the SV to be displaced from the beam spot (defined as the average interaction point in the plane transverse to the beams) and the displacement vector to be aligned with the dimuon momentum.”

Example of $B^+ \rightarrow J/\psi (\mu^+ \mu^-) K^+$ in CMS


- Early 8 TeV result



Test of Use of Future Absolute B_s Branching Fraction for Normalization

- “We also estimate the branching fractions using the $B_s^0 \rightarrow J/\psi\phi(1020)$ decays for the normalization.
- While this result is free from the explicit systematic uncertainty in the f_s/f_u ratio, it depends on the $B_s^0 \rightarrow J/\psi\phi(1020)$ branching fraction.
 - At the moment, this branching fraction measurement uses the f_s/f_u ratio measurement as an input, but this dependence may be eliminated when new independent measurements of the $B_s^0 \rightarrow J/\psi\phi(1020)$ branching fraction become available, such as the measurement planned by the Belle II Collaboration at the KEKB e^+e^- collider [using the $Y(5S)$ data. Experimentally, the measurement based on the $B_s^0 \rightarrow J/\psi\phi(1020)$ normalization channel has slightly larger systematic uncertainties due to the presence of the second kaon in the final state.”
 - Work will need to be done to reduce this this source of uncertainty.

Angular analysis of the decay $B^+ \rightarrow K^+ \mu^+ \mu^-$ in proton-proton collisions at $\sqrt{s} = 8$ TeV

The CMS Collaboration 

Abstract

The angular distribution of the flavor-changing neutral current decay $B^+ \rightarrow K^+ \mu^+ \mu^-$ is studied in proton-proton collisions at a center-of-mass energy of 8 TeV. The analysis is based on data collected with the CMS detector at the LHC, corresponding to an integrated luminosity of 20.5 fb^{-1} . The forward-backward asymmetry A_{FB} of the dimuon system and the contribution F_{H} from the pseudoscalar, scalar, and tensor amplitudes to the decay width are measured as a function of the dimuon mass squared. The measurements are consistent with the standard model expectations.

Published in *Physical Review D* as [doi:10.1103/PhysRevD.98.112011](https://doi.org/10.1103/PhysRevD.98.112011).

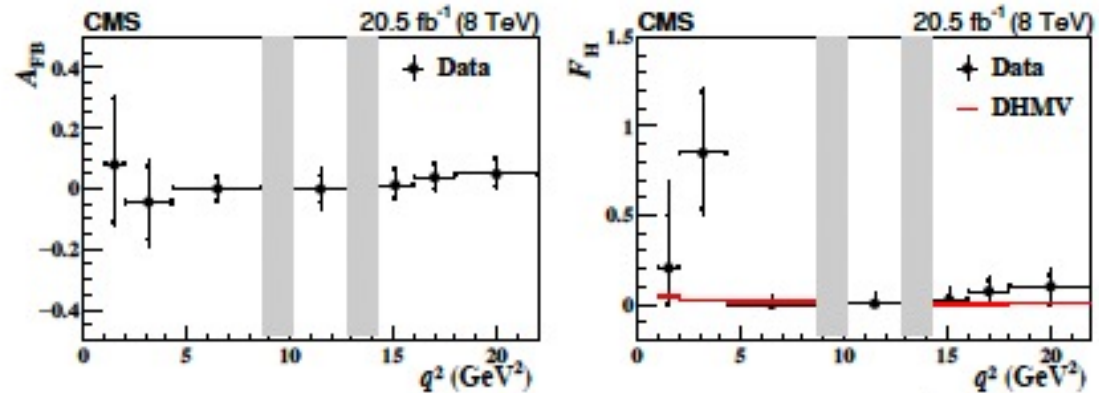
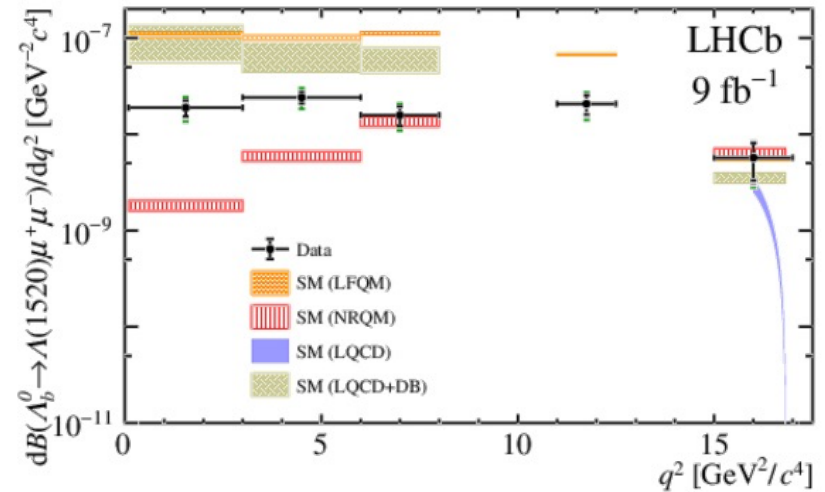
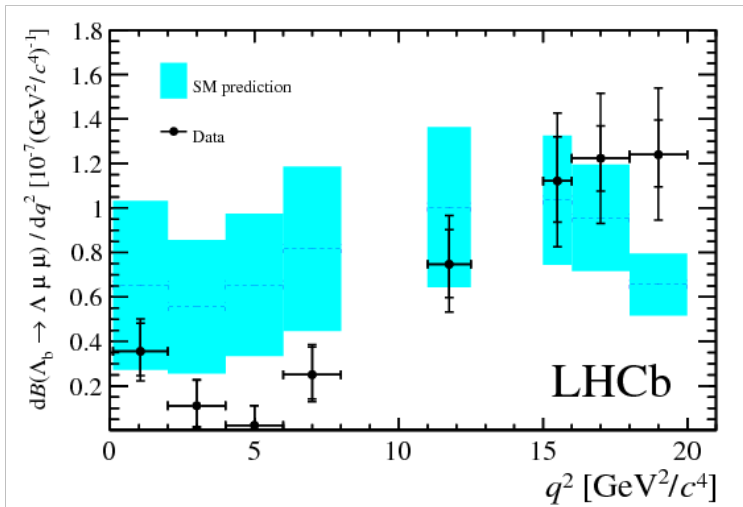
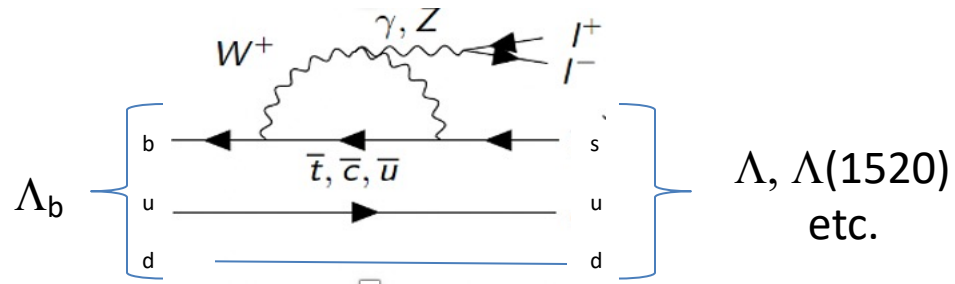


Figure 5: Results of the A_{FB} (left) and F_{H} (right) measurements in ranges of q^2 . The statistical uncertainties are shown by the inner vertical bars, while the outer vertical bars give the total uncertainties. The horizontal bars show the q^2 range widths. The vertical shaded regions are 8.68 – 10.09 and 12.86 – 14.18 GeV^2 , corresponding to the J/ψ - and $\psi(2S)$ -dominated control regions, respectively. The horizontal lines in the right plot show the DHMV SM theoretical predictions [32, 33], whose uncertainties are smaller than the line width.

$\Lambda_b \rightarrow \Lambda, \Lambda(1520) (\text{pK}) \mu^+ \mu^-$ from LHCb

[arXiv:2302.08262](https://arxiv.org/abs/2302.08262)

$\Lambda(1520)$: $0(3/2)^-$
 $M = 1519 \text{ MeV}, \Gamma = 16 \text{ MeV}$
 $\mathcal{B}(\text{pK}) = 22.5\%$



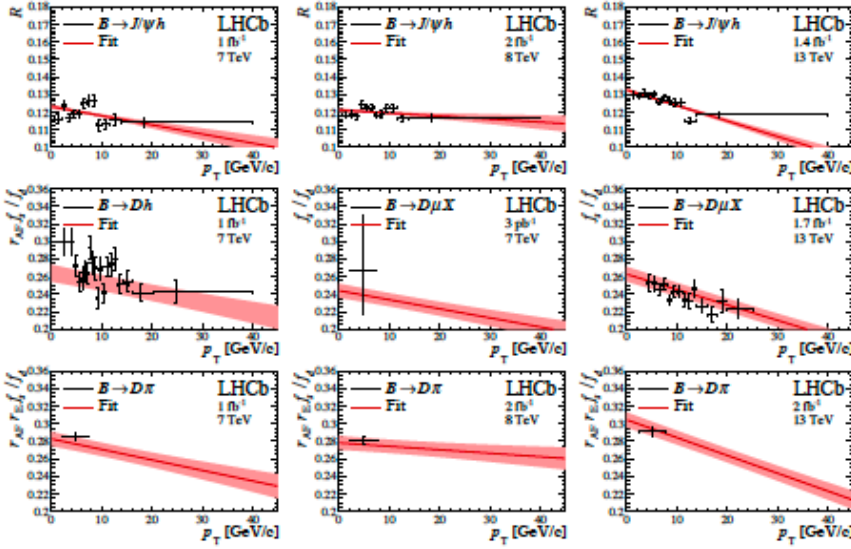


Figure 1: Measurements of f_s/f_d sensitive observables as a function of the B -meson transverse momentum, p_T , overlaid with the fit function. The scaling factors r_{AF} and r_E are defined in the text; the variable \mathcal{R} is defined in Eq. 4. The vertical axes are zero-suppressed. The uncertainties on the data points are fully independent of each other; overall uncertainties for measurements in multiple p_T intervals are propagated via scaling parameters, as described in the text. The band associated with the fit function shows the uncertainty on the post-fit function for each sample.

$$\begin{aligned}
 f_s/f_d(p_T, 7 \text{ TeV}) &= (0.244 \pm 0.008) + ((-10.3 \pm 2.7) \times 10^{-4}) \cdot p_T, \\
 f_s/f_d(p_T, 8 \text{ TeV}) &= (0.240 \pm 0.008) + ((-3.4 \pm 2.3) \times 10^{-4}) \cdot p_T, \\
 f_s/f_d(p_T, 13 \text{ TeV}) &= (0.263 \pm 0.008) + ((-17.6 \pm 2.1) \times 10^{-4}) \cdot p_T.
 \end{aligned}$$

Table 3: Observables and related parameters of the default fit. See text for a detailed explanation.

Observable	Parameters	Fit mode
f_s/f_d	$a(7 \text{ TeV}), a(8 \text{ TeV}), a(13 \text{ TeV})$ $b(7 \text{ TeV}), b(8 \text{ TeV}), b(13 \text{ TeV})$	Free
$B(B_s^0 \rightarrow D_s^- \pi^+)$	r_{AF}	Gaussian constrained
	r_E	Gaussian constrained
$B(B_s^0 \rightarrow J/\psi \phi)$	\mathcal{F}_R	Free
	S_1	Gaussian constrained
	S_2, S_3, S_4	Gaussian constrained

$S_2, S_3,$ and $S_4,$ the parameters propagating experimental systematic uncertainties on the input measurements.

$$\begin{aligned}
 f_s/f_d(p_T, 7 \text{ TeV}) &= (0.244 \pm 0.008) + ((-10.3 \pm 2.7) \times 10^{-4}) \cdot p_T, \\
 f_s/f_d(p_T, 8 \text{ TeV}) &= (0.240 \pm 0.008) + ((-3.4 \pm 2.3) \times 10^{-4}) \cdot p_T, \\
 f_s/f_d(p_T, 13 \text{ TeV}) &= (0.263 \pm 0.008) + ((-17.6 \pm 2.1) \times 10^{-4}) \cdot p_T,
 \end{aligned}$$

$$B(B_s^0 \rightarrow J/\psi \phi, \phi \rightarrow K^+ K^-) = (5.01 \pm 0.16 \pm 0.17) \times 10^{-4}$$

$$B(B_s^0 \rightarrow J/\psi \phi) = (1.018 \pm 0.032 \pm 0.037) \times 10^{-3},$$

Precise measurement of the f_s/f_d ratio of fragmentation fractions and of B_s^0 decay branching fractions

LHCb collaboration[†]

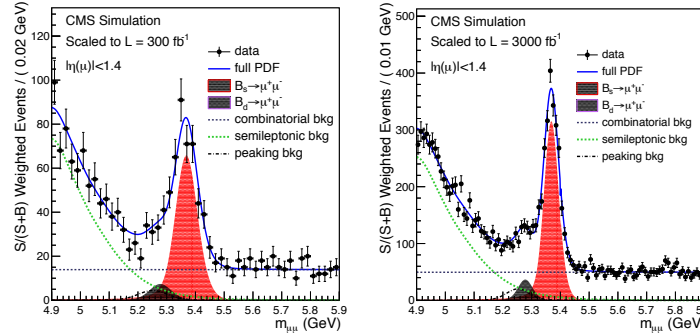
Abstract

The ratio of the B_s^0 and B^0 fragmentation fractions, f_s/f_d , in proton-proton collisions at the LHC, is obtained as a function of B -meson transverse momentum and collision centre-of-mass energy from the combined analysis of different B -decay channels measured by the LHCb experiment. The results are described by a linear function of the meson transverse momentum, or with a function inspired by Tsallis statistics. Precise measurements of the branching fractions of the $B_s^0 \rightarrow J/\psi \phi$ and $B_s^0 \rightarrow D_s^- \pi^+$ decays are performed, reducing their uncertainty by about a factor of two with respect to previous world averages. Numerous B_s^0 decay branching fractions, measured at the LHCb experiment, are also updated using the new values of f_s/f_d and branching fractions of normalisation channels. These results reduce a major source of systematic uncertainty in several searches for new physics performed through measurements of B_s^0 branching fractions.

Published in Phys. Rev. D104 (2021) 032005

Forecast

→ Next target is
 $B_d \rightarrow \mu^+ \mu^-$



Notice better mass resolution in CMS for HL-LHC

Figure 3: Projections of the mass fits to 300 fb^{-1} (left) and 3000 fb^{-1} (right) of integrated luminosity (L), respectively assuming the expected performances of Phase-I and Phase-II CMS detectors.

$\mathcal{L} \text{ (fb}^{-1}\text{)}$	Estimate of analysis sensitivity					
	$N(B_s^0)$	$N(B^0)$	$\delta\mathcal{B}(B_s^0 \rightarrow \mu^+ \mu^-)$	$\delta\mathcal{B}(B^0 \rightarrow \mu^+ \mu^-)$	$B^0 \text{ sign.}$	$\delta \frac{\mathcal{B}(B^0 \rightarrow \mu^+ \mu^-)}{\mathcal{B}(B_s^0 \rightarrow \mu^+ \mu^-)}$
20	18.2	2.2	35%	> 100%	$0.0 - 1.5 \sigma$	> 100%
100	159	19	14%	63%	$0.6 - 2.5 \sigma$	66%
300	478	57	12%	41%	$1.5 - 3.5 \sigma$	43%
300 (barrel)	346	42	13%	48%	$1.2 - 3.3 \sigma$	50%
3000 (barrel)	2250	271	11%	18%	$5.6 - 8.0 \sigma$	21%

Observable	Current	LHCb-U1a	LHCb-U2	ATLAS	CMS
$\mathcal{B}(B_s^0 \rightarrow \mu^+ \mu^-) (\times 10^9)$	± 0.46	± 0.30	± 0.16	$\pm (0.50)$	± 0.39
$\frac{\mathcal{B}(B^0 \rightarrow \mu^+ \mu^-)}{\mathcal{B}(B_s^0 \rightarrow \mu^+ \mu^-)}$	$\sim 70\%$	$\sim 34\%$	$\sim 10\%$	—	$\sim 21\%$
$\tau_{\mu\mu}$	$\sim 14\%$	$\pm 0.16 \text{ ps}$	$\pm 0.04 \text{ ps}$	—	$\pm 0.05 \text{ ps}$

Table 3: Summary of the current and expected experimental precision for $B_s^0 \rightarrow \mu^+ \mu^-$ and $B^0 \rightarrow \mu^+ \mu^-$ observables. The expected uncertainty are reported for LHCb at 23 fb^{-1} (LHCb-U1a) and 300 fb^{-1} (LHCb-U2) while for ATLAS and CMS are evaluated at 3 ab^{-1} .

BELLE Branching Fraction Measurements on $\Upsilon(5S)$

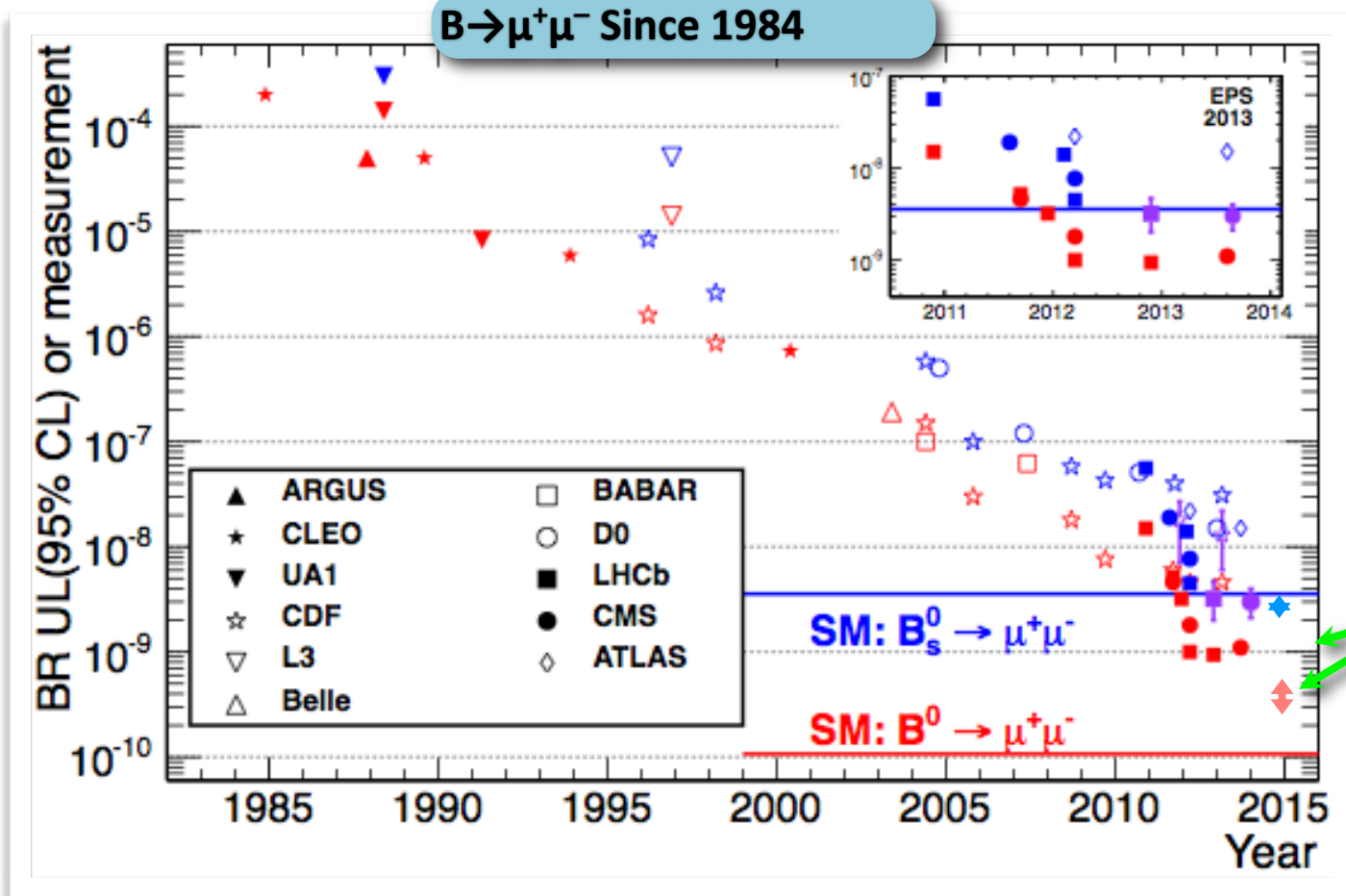
[17] Belle collaboration, F. Thorne *et al.*, *Measurement of the decays $B_s^0 \rightarrow J/\psi \phi(1020)$, $B_s^0 \rightarrow J/\psi f_2'(1525)$ and $B_s^0 \rightarrow J/\psi K^+ K^-$ at Belle*, [Phys. Rev. D88 \(2013\) 114006](#), [arXiv:1309.0704](#)

We report a measurement of the branching fraction of the decay $B_s^0 \rightarrow J/\psi \phi(1020)$, evidence and a branching fraction measurement for $B_s^0 \rightarrow J/\psi f_2'(1525)$, and the determination of the total $B_s^0 \rightarrow J/\psi K^+ K^-$ branching fraction, including the resonant and non-resonant contributions to the $K^+ K^-$ channel. We also determine the S -wave contribution within the $\phi(1020)$ mass region. The absolute branching fractions are $\mathcal{B}[B_s^0 \rightarrow J/\psi \phi(1020)] = (1.25 \pm 0.07 \text{ (stat)} \pm 0.08 \text{ (syst)} \pm 0.22 (f_s)) \times 10^{-3}$, $\mathcal{B}[B_s^0 \rightarrow J/\psi f_2'(1525)] = (0.26 \pm 0.06 \text{ (stat)} \pm 0.02 \text{ (syst)} \pm 0.05 (f_s)) \times 10^{-3}$ and $\mathcal{B}[B_s^0 \rightarrow J/\psi K^+ K^-] = (1.01 \pm 0.09 \text{ (stat)} \pm 0.10 \text{ (syst)} \pm 0.18 (f_s)) \times 10^{-3}$, where the last systematic error is due to the branching fraction of $b\bar{b} \rightarrow B_s^{(*)} B_s^{(*)}$. The branching fraction ratio is found to be $\mathcal{B}[B_s^0 \rightarrow J/\psi f_2'(1525)]/\mathcal{B}[B_s^0 \rightarrow J/\psi \phi(1020)] = (21.5 \pm 4.9 \text{ (stat)} \pm 2.6 \text{ (syst)})$. All results are based on a 121.4 fb^{-1} data sample collected at the $\Upsilon(5S)$ resonance by the Belle experiment at the KEKB asymmetric-energy e^+e^- collider.

$$(1.25 \pm 0.07 \pm 0.23) \times 10^{-3} |$$

This seems to use f_s to get the BR!

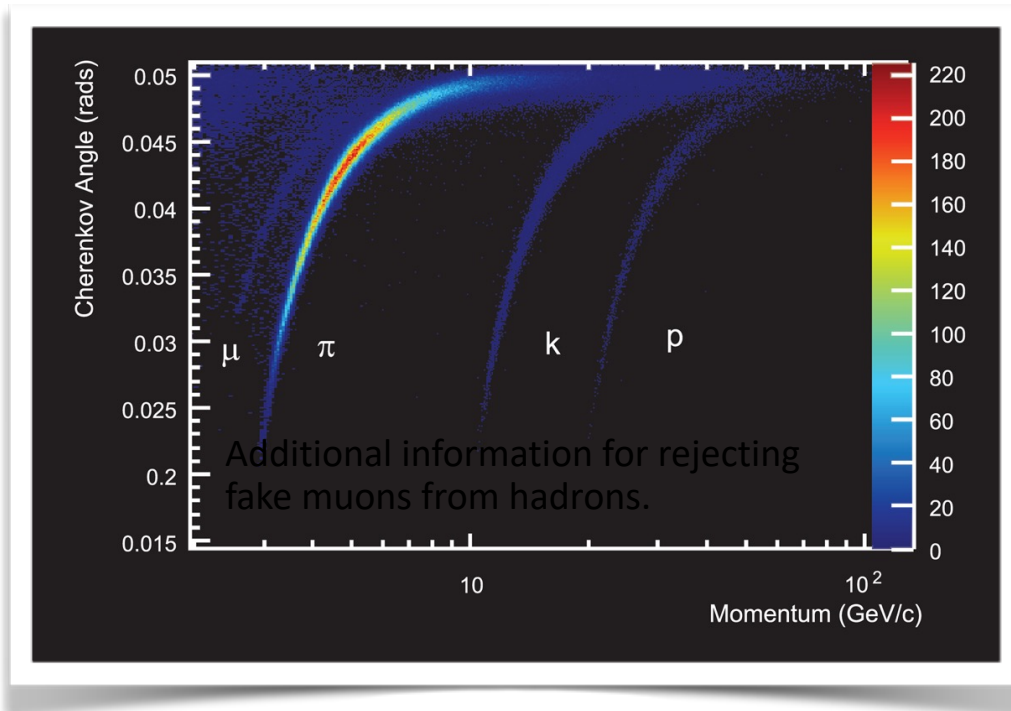
Historical Summary



It took 30 years to finally measure the $B_s \rightarrow \mu^+ \mu^-$ decay; The result turns out to be very close to the prediction and gives a stringent limit on the physics beyond the Standard Model. There is still a possibility of $\sim 50\%$ deviation from the SM, which will be resolved by more statistics in the next few years.

LHCb PARTICLE ID

- LHCb has a dedicated (active) particle identification device: RICH (Ring Imaging Cherenkov) detector.
- **A global particle ID likelihood** is constructed based on the information from the **RICH** detectors, calorimeters (**CALO**), and **MUON** system.



**Powerful muon identification with high (~98%) efficiency:
Based on muon chambers information + the global PID likelihood:**

$$\epsilon(\pi \rightarrow \mu) \sim 0.6\%$$

$$\epsilon(K \rightarrow \mu) \sim 0.4\%$$

$$\epsilon(p \rightarrow \mu) \sim 0.3\%$$

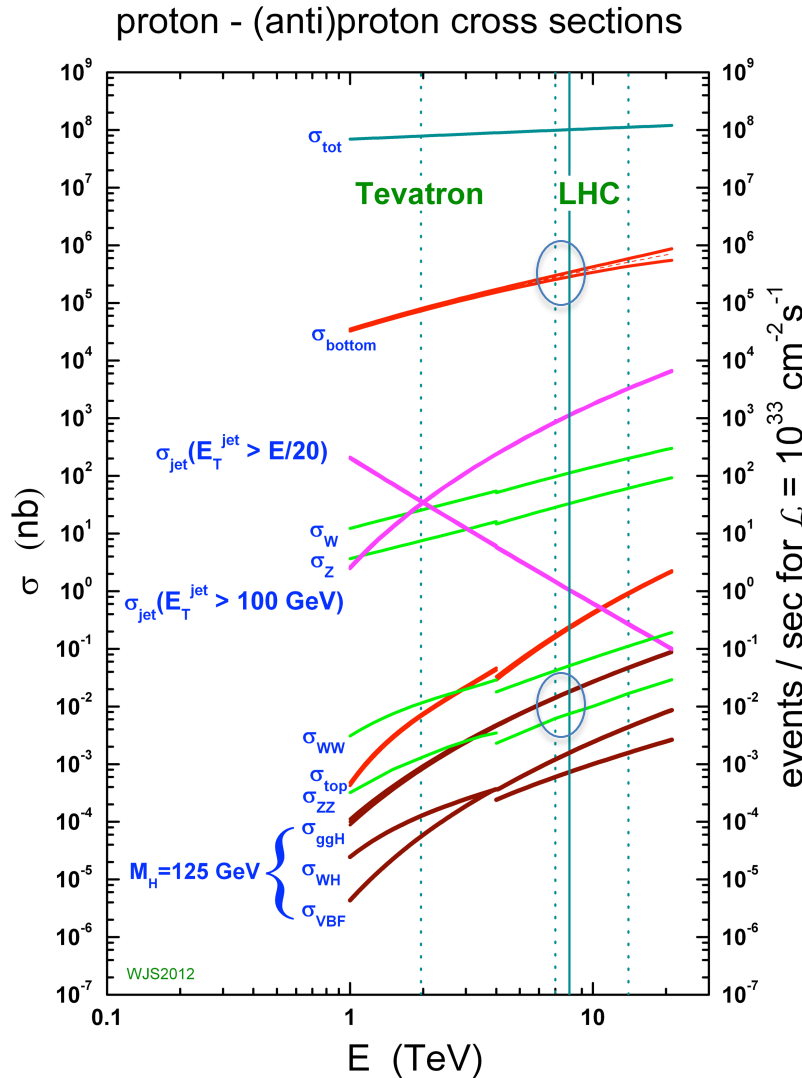
Some B_s , B_d meson properties

- The B_s meson is a $\bar{b}s$ bound state; the B_d meson is a $\bar{b}d$ bound state
- The Mass of the B_s is $5366.7 \text{ MeV}/c^2$ and the B_d is $5279.55 \text{ MeV}/c^2$
 - $M_{B_s} - M_{B_d} = \sim 87 \text{ MeV}/c^2$
- B_s^0 is a flavor eigenstate, not a mass eigenstate, and oscillates rapidly between B_s and \bar{B}_s
- The interactions that produce mixing also can produce a difference in lifetimes between the two mass eigenstates B_{sH} and B_{sL} of about 10%
- The B_d^0 has weaker mixing, oscillates more slowly and there is almost no difference in the lifetimes of its two mass eigenstates
- Both B_d and B_s have mean lifetimes of 1.5ps, corresponding to $c\tau$ of $\sim 450\mu \text{ m}$
- The distance from the production (primary) vertex to the B decay (secondary) vertex can be measured and used to eliminate most prompt backgrounds

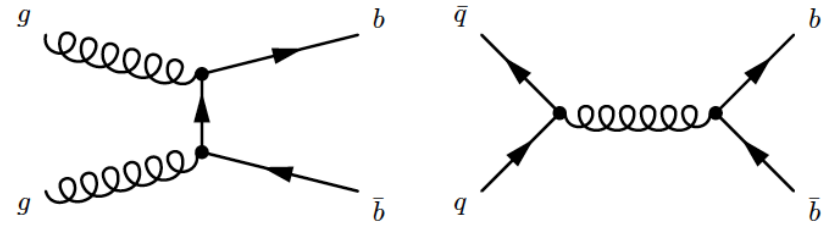
Review: Properties of B_s and B_d

Property	B_d	B_s	Comment
Mass (MeV)	5279.55	53667.7	$M_{B_s} - M_{B_d} = 87.34$
$\Delta M_{B_d} (10^{12} \text{ h}/2\pi \text{ s}^{-1})$	0.510		$\Delta [M(B_{dH}^0) - M(B_{dL}^0)]$
$\Delta M_{B_s} (10^{12} \text{ h}/2\pi \text{ s}^{-1})$		17.769	$\Delta [M(B_{sH}) - M(B_{sL})]$
Mean Lifetime (ps)	1.519	1.469	
B_{sH} mean life (ps)		1.70	
$\Delta \Gamma (B_d) (\text{ps}^{-1})$	$(42 \pm 10) \times 10^{-4} \Gamma$		$\Delta \Gamma(B_d) = \Gamma(B_{dL}) - \Gamma(B_{dH})$
$\Delta \Gamma (B_s) (\text{ps}^{-1})$		0.091 ± 0.016	$\Delta \Gamma(B_s) = \Gamma(B_{sL}) - \Gamma(B_{sH})$
$\Delta M/\Gamma (B_d)$	0.774		
$\Delta M/\Gamma (B_s)$		26.85	

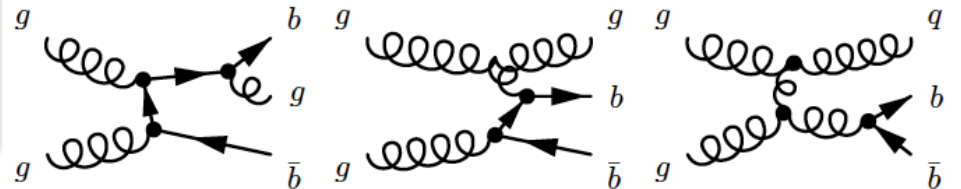
B Production at the LHC is large



LO – Pair creation



NLO –
pair creation, Flavor Excitation, Gluon splitting



Observable	Current	LHCb-U1a	LHCb-U2	ATLAS	CMS
$\mathcal{B}(B_s^0 \rightarrow \mu^+ \mu^-) (\times 10^9)$	± 0.46	± 0.30	± 0.16	$\pm (0.50)$	± 0.39
$\frac{\mathcal{B}(B^0 \rightarrow \mu^+ \mu^-)}{\mathcal{B}(B_s^0 \rightarrow \mu^+ \mu^-)}$	$\sim 70\%$	$\sim 34\%$	$\sim 10\%$	–	$\sim 21\%$
$\tau_{\mu\mu}$	$\sim 14\%$	± 0.16 ps	± 0.04 ps	–	± 0.05 ps

Table 3: Summary of the current and expected experimental precision for $B_s^0 \rightarrow \mu^+ \mu^-$ and $B^0 \rightarrow \mu^+ \mu^-$ observables. The expected uncertainty are reported for LHCb at 23 fb^{-1} (LHCb-U1a) and 300 fb^{-1} (LHCb-U2) while for ATLAS and CMS are evaluated at 3 ab^{-1} .

This is after Moriond 2021 so does not contain all recent results, view as illustrative only

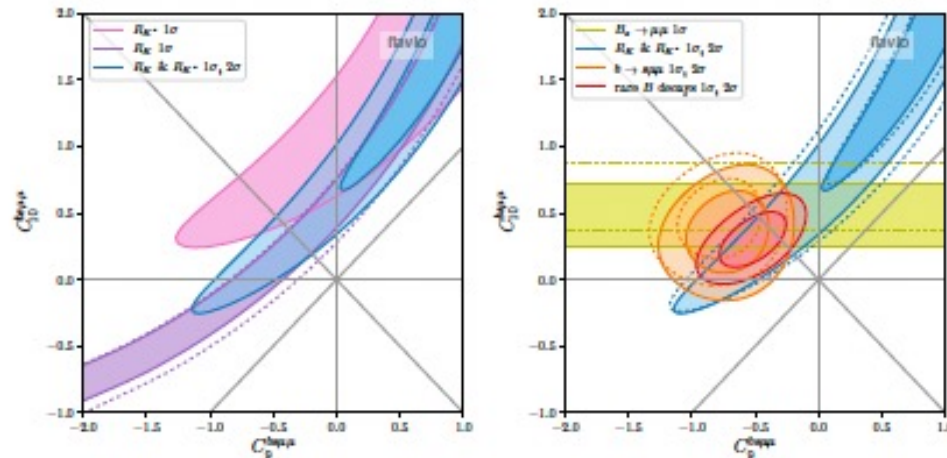


Figure 4: Constraints in the Wilson coefficient plane $C_9^{\delta\mu\mu}$ vs. $C_{10}^{\delta\mu\mu}$. Left: LFU ratios only. Right: Combination of LFU ratios, combination of $b \rightarrow s\mu\mu$ observables, $\text{BR}(B_s \rightarrow \mu^+ \mu^-)$, and the global fit. The dashed lines show the constraints before the recent updates [11, 13, 14, 41].

<https://arxiv.org/abs/2103.13370v3>

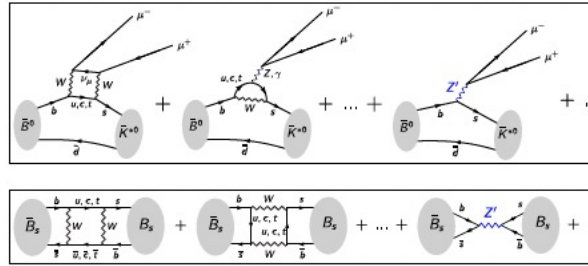


Figure 3: Schematic representation of the (top) $\bar{B}^0 \rightarrow \bar{K}^{*0} \mu^+ \mu^-$ decay and (bottom) B_s^0 - \bar{B}_s^0 mixing amplitudes as sums over all possible Feynman diagrams. The diagrams on the left are examples of SM contributions, while the diagram on the right is an example of an NP contribution in theories with a flavor-changing neutral gauge boson Z' .

This is after Moriond Snowmass 2021 so does not contain all recent results, view as illustrative only

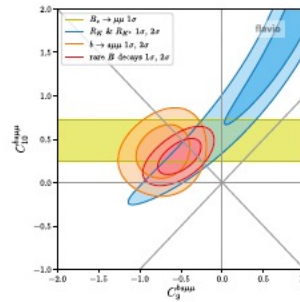
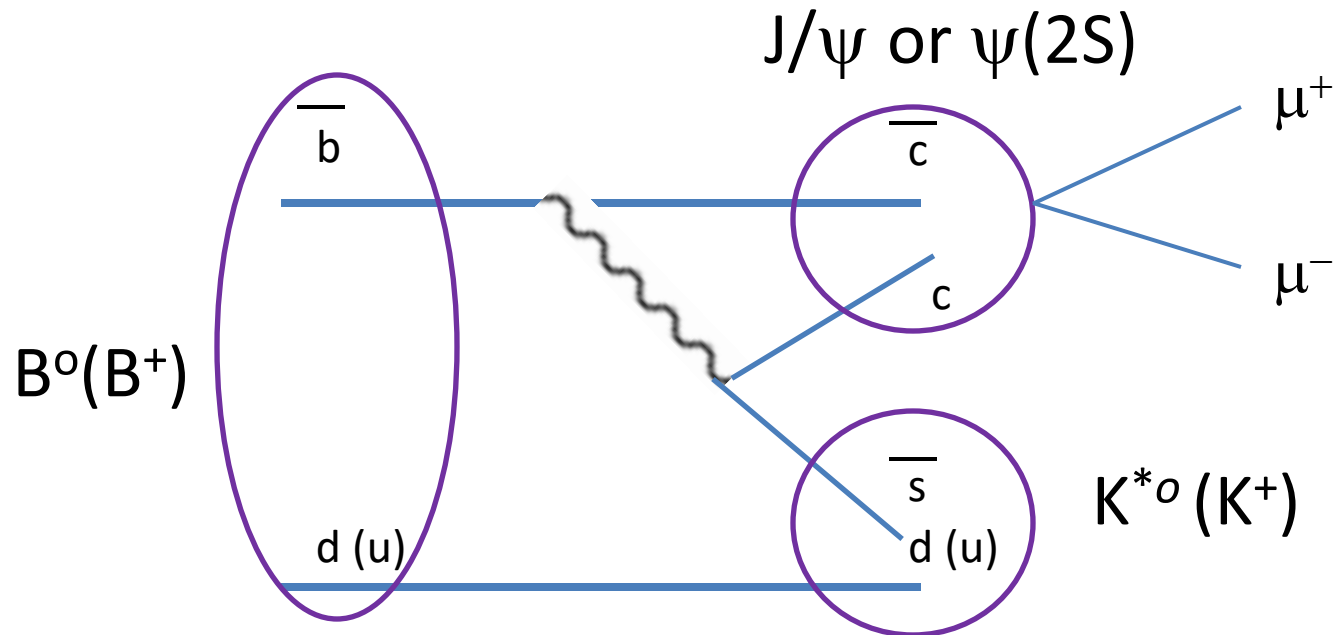


Figure 1: Constraints at 1σ (darker) and 2σ (lighter) in the plane C_9^{bsm} vs. C_{10}^{bsm} resulting from $\mathcal{B}(B_s^0 \rightarrow \mu^+ \mu^-)$ (yellow-green), combination of the lepton-flavor-universality ratios R_K and R_{K^*} (blue), combination of $b \rightarrow s \mu^+ \mu^-$ observables (orange), and global fit of rare b decays (red) [9]. The Wilson coefficients C_9^{bsm} and C_{10}^{bsm} are the NP contributions to the couplings of the operators $O_9 = (\bar{s} \gamma_\mu b_L)(\bar{\mu} \gamma^\mu \mu)$ and $O_{10} = (\bar{s} \gamma_\mu b_L)(\bar{\mu} \gamma^\mu \gamma_5 \mu)$, respectively. The global fit result is inconsistent with the SM point (the origin) by $\sim 5\sigma$.

<https://arxiv.org/abs/2208.05403v2>



The anti-b quark does not decay through a loop diagram. These are CKM and Cabibbo favored decays that, far from being suppressed, have high branching fractions. The J/ψ or $\psi(2S)$ decay into a $\mu^+\mu^-$ creates the resonant contribution that is excluded by the q^2 cuts in the $B^0 \rightarrow K^{*0} \mu^+\mu^-$ analysis. The B^+ is used as a normalization channel in the $B_{s,d} \rightarrow \mu^+\mu^-$ for its similarity to the signal decay (one extra particle, same muon content).